QUEST FOR ANTIMICROBIAL AGENT: FROM NANOPARTICLE TO COMPUTATIONAL BIOLOGY (ANTIMICROBIAL RESISTANCE ELEMENT Cfr AS THE TARGET PROTEIN)

M.Sc. Thesis
2024

Submitted to
Central Department of Biotechnology,
Tribhuvan University,
Kirtipur, Kathmandu, Nepal

By
Pooja Shrestha
Registration No: 5-2-37-2178-2014

Supervisors
Asst. Prof. Alina Shri Sapkota
Dr. Pramod Aryal

ACKNOWLEDGEMENT

I would like to express my special thanks of gratitude to my **supervisors Asst. Prof. Alina Shri Sapkota and Dr. Pramod Aryal** for their valuable guidance and perpetual support. They consistently showed me the right path when I ran into any problem during my entire thesis period and taught me the true essence of perseverance in research and Science. I thank my supervisor Asst. Prof. Alina Shri Sapkota for her faith, love and encouraging words when I fell short of motivation. I am also thankful to **Prof Dr. Krishna Das Manandhar,** Head of Department of Central Department of Biotechnology, Tribhuvan University for letting me complete my thesis works at TU. I express my sincere gratitude towards **Assoc. Prof. Khaga Raj Sharma** from Central Department of Chemistry for nanoparticle characterization facility, and **my friends Ishmita Lohani and Mansa Bhushal** for their assistance. Additionally, I would like to thank the **'University Grants Commission'** for funding my Msc. Thesis research work under the award no. **MRS-78-79-S&T-01**, without which this work wouldn't be possible. Furthermore, generous thanks to my teammates **Jeshika Thapa, Binita Khadka, Ashish Pokhrel, Alisha Nepali, and Sujata Pokhrel** for being there when needed.

I would also like to acknowledge my seniors **Ms. Pooja Pathak, Mr. Samiran Subedi, Ms. Sita Ghimire, Ms. Guheshwori Chataut, Ms. Bisheshta Nepal, and Mr. Bishal Gurung,** for assisting and guiding when required. Heartfelt thanks to all my friends including **Sujeeta Maharjan, Shobha Amagain, Pragya Sapkota and Puja Dahal** for their consistent assistance and support.

Last but not the least, I must express my earnest gratitude to my '**Parents'** for providing me continued help and support throughout all these years and through the process of research works and writing this thesis. Thanks for all your encouragement, incredible patience and faith in me.

Pooja Shrestha.

LIST OF ABBREVIATIONS

ADMET	Absorption, Distribution, Metabolism, Excretion and Toxicity
AgNP	Silver Nanoparticle
AMR	Antimicrobial Resistance
AST	Antimicrobial Susceptibility Testing
ATP	Adenosine Triphosphate
BLAST	Basic Local Alignment Search Tool
CADD	Computer Aided Drug Designing
Cfr	Chloramphenicol-Florfenicol Resistance
COVID-19	Corona Virus of 2019
DNA	Deoxyribonucleic Acid
FTIR	Fourier Transform Infrared Spectroscopy
HTS	High Throughput Screening
ISP	International *Streptomyces* Project
LBVS	Ligand-Based Virtual Screening
MDR	Multi-Drug Resistance
MBC	Minimum Bactericidal Concentration
MIC	Minimum Inhibitory Concentration
µg	Microgram
µl	Microliter
mM	Millimolar
Nm	Nanometer

NCBI	National Center for Biotechnology Information
NMR	Nuclear Magnetic Resonance
PDB	Protein Data Bank
PDR	Pan Drug Resistance
$PhLOPS_A$	Phenicol, Lincosamide, Oxazolidinones, Pleuromutilins and Streptogramin A
PCR	Polymerase Chain Reaction
TPSA	Total Polar Surface Area
ROS	Reactive Oxygen Species
rRNA	Ribosomal Ribonucleic Acid
RlmN	Ribosomal RNA large subunit Methyltransferase N
SAM	S-Adenosyl Methionine
SAH	S-Adenosyl L-Homocysteine
SBVS	Structure Based Virtual Screening
SPR	Surface Plasmon Resonance
Tox	Toxicity
tPSA	Topological Polar Surface Area
VS	Virtual Screening
WHO	World Health Organization
XDR	Extensive Drug Resistance

LIST OF TABLES

S.No.	Table No.	Page No.	Name of the table
1	1	12	Sample collection area
2	2	13	Modified media composition
3	3	13	Mineral mix composition
4	4	13	Vitamin mix composition
5	5	15	ISP4 broth composition
6	6	16	Starch Casein Broth composition
7	7	18	PCR Mixture composition
8	8	18	PCR conditions
9	9	21	ADME/Tox Filter
10	10	22	Molecular Docking reference values for filter proteins
11	11	23	Molecular Docking reference values for target proteins
12	12	26	Biochemical enzymatic assay
13	13	26	Carbohydrate Utilization test
14	14	28	ATCC strains AST standardization
15	15	36	Binding affinity of prioritized hits against target Cfr
16	16	38	Ligand-protein interaction of top hit ligands
17	17	40	Ligand-protein interaction bond types of top hit ligands

LIST OF FIGURES

S.No.	Figure No.	Page No.	Name of the figure
1	1	16	Separating funnel
2	2	16	Antibiotic concentration in rotary evaporator
3	3	24	Spread plate in modified media
4	4	25	Gram Staining under 100X magnification
5	5	25	Enzymatic assay
6	6	25	Nitrate Reduction Test
7	7	26	Carbohydrate Utilization test
8	8	27	Perpendicular streak plate technique for primary screening
9	9	27	Secondary metabolite production
10	10	27	Antibiotic crude extract
11	11	27	Biogenic AgNP synthesis
12	12	28	Antimicrobial susceptibility plate assay
13	13	28	Determination of the MIC and MBC by resazurin based microdilution method of I53 extract
14	14	29	Molecular characterization of isolate- gDNA and PCR product band
15	15	30	Phylogenetic tree of *Streptomyces* isolate I53
16	16	31	UV–Visible spectrum of silver nanoparticles
17	17	32	Fourier transform infrared spectroscopy analysis of AgNP
18	18	32	Determination of the MIC and MBC by resazurin based microdilution method of AgNP
19	19	33	3D structure of Cfr obtained using Alphafold2
20	20	33	Predicted aligned Error plot of predicted structure of CFR

21	21	34	RlmN and CFR structure alignment using Pymol
22	22	34	RlmN and CFR sequence alignment using Clustal omega
23	23	35	3D structure validation
24	24	37	Structure of Lead compounds
25	25	37	Cfr protein interaction within $5A^0$ with hit compounds
26	26	39	Bond types in interaction with hit compounds
27	27	40	Hydrophobic interaction of residues with hits using Ligplot+

Table of Contents

ACKNOWLEDGEMENT iv

LIST OF ABBREVIATIONS v

LIST OF TABLES vii

LIST OF FIGURES viii

ABSTRACT xi

1. INTRODUCTION 1

1.1 Background 1

1.2 Current studies 2

1.3 HYPOTHESIS 4

1.3.1 Null Hypothesis 4

1.3.2 Alternate Hypothesis: 4

1.4 OBJECTIVE 4

1.4.1 General objective 4

1.4.2 Specific objectives 4

1.5 RATIONALE 4

1.6 SCOPE 4

2. LITERATURE REVIEW 5

2.1 Antibiotic history 5

2.1.1 Antibiotic producers 5

2.1.2 Genus: *Streptomyces* 6

2.1.3 Bioactive secondary metabolite production 6

2.1.4 Biogenic AgNP synthesis 7

2.2 Target modification: An antimicrobial resistance mechanism 8

2.2.1 Cfr as a target 8

2.2.2 Antimicrobial potentiators 9

2.3 Computer Aided Drug Designing 9

2.3.1 Virtual Screening of potentiators with druggable Properties 10

2.3.2 Molecular Docking 10

3. MATERIALS AND METHODS 12
3.1 Materials, organisms and chemicals used in the study 12
3.2 Secondary metabolite antibacterial efficacy testing 12
3.2.1 Selection of soil samples and sample collection 12
3.2.2 Soil treatment, media selection and primary culture 12
3.2.3 Macroscopic colony study and pure culture isolation 13
3.2.4 Colony identification by Morphology and Gram staining 14
3.2.5 Enzymatic Assay 14
3.2.5.1 Starch Hydrolysis test 14
3.2.5.2 Cellulose Hydrolysis test 14
3.2.5.3 Gelatin Hydrolysis test 14
3.2.5.4 Carbohydrate Utilization test 14
3.2.5.5 Nitrate Reduction test 15
3.2.6 Primary screening against ATCC test pathogens 15
3.2.7 Secondary metabolite production 15
3.2.7.1 Antibiotic extraction 16
3.2.7.2 Antimicrobial susceptibility plate assay 16
3.2.7.3 Resazurin antimicrobial assay for MIC MBC determination 17
3.2.8 Molecular characterization of isolate 17
3.2.8.1 16S rRNA amplification 18
3.2.8.2 Sequencing, alignment and phylogenetic tree construction 18
3.3 Antibacterial efficacy testing of biogenic AgNP 19
3.3.1 Silver nanoparticle synthesis 19
3.3.2 UV-vis spectrophotometer analysis 19
3.3.3 AgNP FTIR characterization 19
3.3.4 Resazurin antimicrobial assay for MIC MBC determination 19
3.4 In Silico potentiator screening against Cfr 19
3.4.1 Target selection 19
3.4.1.1 3D crystal structure search and building 19
3.4.1.2 Target 3D structure validation 20
3.4.1.3 Protein preparation 20

3.4.2 Ligand library Preparation 20
3.4.2.1 ADME/TOX filter 20
3.4.2.2 Protein and ligand library preparation in dockable format 21
3.4.3 Molecular Docking 21
3.4.3.1 Filter 1: Docking against HMAT protein 21
3.4.3.2 Filter 2: Docking against human cytochrome p450 Cyp3A4 protein 22
3.4.3.3 Dock 1: Setting reference values for docking 22
3.4.3.4 Dock 2: Final docking against target protein Cfr 23
3.4.4 Docking result analysis 23
3.4.4.1 Interactions of ligands and protein target 23
3.4.4.2 Bond type visualization and analysis 23
3.4.4.3 Hydrophobic bond interactions 23
4. RESULTS AND DISCUSSION 24
4.1 Secondary metabolite activity testing 24
4.1.1 Primary culture, colony study and isolation 24
4.1.2 Macroscopic colony identification and gram staining 24
4.1.3 Enzymatic Assay 25
4.1.4 Primary screening 27
4.1.5 Secondary metabolites and AgNP production 27
4.1.5.1 Antibiotic extraction 27
4.1.5.2 Antimicrobial susceptibility plate assay 28
4.1.5.3 Resazurin antimicrobial assay of secondary metabolite 28
4.1.6 Molecular characterization of isolate 29
4.1.6.1 16S rRNA amplification 29
4.1.6.2 Sequence alignment and phylogenetic tree construction 30
4.2 Biogenic AgNP activity testing 31
4.2.1 UV-vis spectrophotometer analysis 31
4.2.2 AgNP FTIR characterization 32
4.2.3 AgNP resazurin antimicrobial assay for MIC MBC determination 32
4.3 In silico potentiator screening against Cfr 33
4.3.1 Target selection and preparation 33

4.3.1.1 3D crystal structure search and building 33
4.3.1.2 Target 3D structure validation 34
4.3.2 Ligand preparation 36
4.3.2.1 ADME/TOX filter 36
4.3.2.2 Filter 1 and Filter 2 36
4.3.3 Molecular Docking against Cfr 36
4.3.4 Docking result analysis 36
4.3.4.1 Interactions of ligands and protein target 37
4.3.4.2 Bond type visualization and analysis 39
4.3.4.3 Hydrophobic bond interactions 40
5. SUMMARY 42
6. CONCLUSION 43
7. RECOMMENDATION 44
8. REFERENCES 45
9. APPENDICES 53

ABSTRACT

Rapid emergence of superbugs at an unprecedented rate is posing great risk to human health. To address this issue, a diversified integrated approach of antibiotic development, scope of nanoparticles and in silico potentiators screening has been explored in this study. In this regard computation biology approach has been taken in consideration for identification of ligands that could be co-administered with the present-day PhLOPS antibiotics, especially chloramphenicol. The screening parameters ADMET was employed to screen ligands with drug-likeness. In addition, the ligand needed to be non-inhibitory to hMAT1A and Cyp450 3A4 due to their role in immunity and drug metabolism, hence molecular docking with these proteins were performed prior to final docking against the resistance element Cfr. The lead compound ZINC72320745 with inhibitory binding affinity against bacterial Cfr enzyme responsible for chloramphenicol clearance in bacteria has a furan scaffold that suggests the saprophytic nature of the *Streptomyces sps*. could be explored further with furfural supplementation in the media. However, in this research, tannic acid incorporated modified media was introduced to isolate robust *Streptomyces*, due to its polyphenolic stress inducing nature. Further, antimicrobials (antibiotic and biogenic nanoparticles) were synthesized and tested against standard pathogens after UV-Vis spectroscopy characterization of silver nanoparticles. The results showed the greater pathogen inhibition with silver nanoparticles than its secondary metabolite. Moreover, the FTIR analysis of the nanoparticle revealed presence of phenol, vinylic ether and imine or oxime group in extract, indicating responsible for its antimicrobial as well as reducing property. The isolate I53 has been found clade forming with *Streptomyces rubiginosohelvolus* strain 183DZ from the phylogenetic analysis suggesting relatedness.

Keywords: *Streptomycetes*, antibiotics, Silver nanoparticle, Molecular docking, Cfr, RlmN, UV-Vis spectroscopy, FTIR

1. INTRODUCTION

1.1 Background

The real story of AMR seems to have begun with the discovery of antibiotics and its antimicrobial inhibition phenomenon. The existence of antibiotics first became known from the famous incident of Sir Alexander Fleming's Penicillin discovery in 1928 from a mold, *Penicillium notatum*. Subsequently, between 1950 and 1970, the novel antibiotic discovery pace quickly picked up, supposedly referring to it as a 'golden antibiotic era'. During this period, discovery of the major classes of antibiotics such as β-lactam antibiotics (including penicillin, cephalosporin, and carbapenem), aminoglycosides (including tobramycin), tetracyclines, macrolides (including erythromycin), glycopeptides (including vancomycin), polymyxins (including colistin), and fluoroquinolones (including ciprofloxacin) (Baker *et al*., 2018) took place. Ever since then, the chemicals have been the basis of human health and well-being. However, with the frequent and haphazard antimicrobial use, the risk of AMR also grew alongside. As a result, cases of rapid pathogen resistance emerged. In the 90s, additional three novel-class antibiotics namely pleuromutilins, oxazolidinones and lipoglycopeptides also entered the market. While it took only about two years and approximately 9 to 16 years to develop resistance against β-lactam classes and other classes respectively (Baker *et al*., 2018), the resistance against the oxazolidinone linezolid followed quickly in 2001 after its introduction to the market in 2000 (Tsiodras *et al*., 2001).

Fast-forward to now, in the 21st century, the drought of effective antibiotics has surfaced as a result of unmonitored spread of resistant pathogens. Regarding this, the antibiotic misuse in the health sector, food industry, agriculture and animal husbandry for temporary relief and economic gains has only mounted the pressure for urgent novel antimicrobial development and discovery. On the contrary, the discovery and development of new drugs have never been a simple or easy process. It is massively resource straining in terms of time, money and decades of expertise and experience. From the preclinical testing to approval for human usage alone, it is indicated to take 10–15 years (Van Norman, 2016), and the costs involved are too expensive (Morgan *et al*., 2011) in order to conduct it in wider-scale. Meanwhile, 0.1% molecules with potential activity proceed to clinical trials in which more than 90% fail human testing (Takahashi & Nakashima, 2018). Hence, the challenge is real, and the task is upheaval. The recent global encounter of COVID-19 has also reflected as well as inflicted the status of AMR. However, on a positive note, the COVID incident has also opened up avenues to antibiotic development as well with the development of molecular and computational approaches to tackle COVID, AMR and alike. Furthermore, the significant improvement in drug development process includes drug repurposing, accelerated drug entities or precursor

identification, development of approval pathways or emergency usage authorization, collaboration amidst related allies as well as inspired exploration of traditional medicines. Moreover, it has assisted in successful adoption and integration of unconventional as well as innovative drug development strategies-technologies and overall holistic approach (Kumar *et al*., 2023).

Since the major source of natural antimicrobial compounds from *Actinomycetes* has been over mined, the search for other alternatives to harness the discovery of novel antibiotics is equally important with simultaneous exploration of *Actinomycetes* for potential novel drug discovery. As a result, the existing antimicrobial discovery trend shows adoption of all kinds of traditional (antibiotic from *Actinomycetes,* fungi and plant extracts), intermediate (synthetic antibiotic chemistry, combination antibiotic therapy, Phage therapy) and modern (Antimicrobial peptide, CRISPR-Cas9, genome mining, computational biology and nanotechnology) approaches adopting every possible technique and technology to fight AMR challenge (Durand *et al*., 2019). Although it has been a long time since a new antibiotic was discovered using traditional methods in more than a 30-year time period (Lewis, 2020), *Actinomycetes* cannot be overlooked as novel antibiotic source since the group has served as the source of two-third, nearly a 61% of existing antimicrobial compounds. In *Actinomycetes* itself, *Streptomyces* is the predominant group contributing to major class antibiotics such as aminoglycosides, chloramphenicol, tetracycline, macrolides, etc. (Oli *et al*., 2021) followed by other 'rare *actinomycetes*' groups namely- *Micromonosporaceae, Pseudonocardiaceae* and *Thermomonosporaceae* with approximately 16% of total antibiotics of *Actinomycetes* origin (K. Tiwari & Gupta, 2011). Therefore, the *Actinomycetes* still remains as a promising source to novel antibiotics which further require more exploration. Overall, the intermediate and modern approaches like nanotechnology and computational antimicrobial research also hold promise for this fight against antimicrobial resistance.

1.2 Current studies

In the realm of antibiotic resistance, the immunocompromised individuals are one of the weak links as they serve as a reservoir of persister drug resistant bacteria and are also the one at higher risk of AMR. The management of MDR pathogens in today's time has become such a daunting task especially in developing countries like ours (Nepal) (Rijal *et al*., 2021) where usage of antibiotics is rampant without proper monitoring and surveillance, posing local and global population to the higher AMR threats. Consequently, resistant pathogens have developed into more resistant Superbugs which has become a constant challenge to cope with, as even the most effective broad-spectrum antibiotics as well as last-resort antibiotics fail to treat common infections from resistant bacteria. The list of last-resort antibiotics as last line of defense in treating antibiotic resistant pathogen infections include tigecycline, polymyxin E (colistin), daptomycin, vancomycin, linezolid (Li

et al., 2022) and carbapenem (Papp-Wallace *et al*., 2011). However, the 2018 WHO report of critically important antimicrobials for human medicine have ranked these antibiotics in the highest (Polymyxins, cephalosporins, glycopeptides and more) and high (carbapenems, lipopeptides, oxazolidinones and more) priority critically important antimicrobials (WHO, 2018) exhibiting the actual challenge at hand. Furthermore, a spike in number of multiple antibiotic resistant pathogens (*Enterobacteriaceae*, *Enterococcus*, *Staphylococcus*, and *Pseudomonas* strains) to the last-resort antibiotics in hospital wastewater samples has aggravated the AMR status (Li *et al*., 2022).

The problem of AMR manifests in 3 distinct levels - firstly, the multidrug resistance (MDR) level, secondly, extensive drug resistance (XDR) and lastly most threatening pan-drug resistance (PDR). When pathogens are non-susceptible to at least one agent in three or more antimicrobial classes, it is simply referred to as MDR; and if non-susceptibility to at least one agent in all, except two or fewer antimicrobial categories, then it's referred as XDR. Similarly, in case the pathogens are non-susceptible to all antimicrobial agents from all available classes, it is referred to as PDR (Tiwari *et al*., 2021). A series of resistance mechanism has been reported in WHO priority pathogenic bacteria such as carbapenem resistant *Acinetobacter baumannii, Pseudomonas aeruginosa* and *Enterobacteriaceae;* 3rd generation cephalosporin resistant *Klebsiella pneumonia, Escherichia coli* and *Enterobacter spp;* methicillin resistant-Vancomycin intermediate and resistant *Staphylococcus aureus;* vancomycin resistant *Enterococcus faecium* and more (WHO, 2017). The several resistance mechanisms reported include target access prevention (reduced permeability, antibiotic efflux), target mutation (single point mutation, multiple gene copies, possession of homologous functional gene to original target), Target modification (methylation of amino acids and proteins of target), and antibiotic modification (hydrolysis, addition of chemical groups). Similarly, diverse approaches have been adopted to counter them such as combination drug therapy, Bacteriophage therapy, antimicrobial potentiators, targeted nano-tech drug delivery, Molecular docking and more. On the contrary, few side effects (aminoglycoside nephrotoxicity) of strategies like combination drug therapy and regulatory guidelines (phage therapy with shortcomings of lowered effectiveness of specific phages when used in mixtures and possibility of phage aiding in DNA transfer within the bacterial community) has become a challenge or rather impediment. (Moo *et al*., 2020).

Moreover, the recent COVID incidence has sidelined the significance of antibiotics to quite an extent shifting focus to the vaccines even with regards to bacterial infection and its treatment procedures. While antibiotics and vaccines have been the traditional ways to treat infection for the longest period of time, the significance of antibiotics is larger than vaccines overall because it capacitates modern medicine. The highly sensitive medical procedures like surgery, chemotherapy, or organ transplantation tend to become highly problematic without the availability of efficient antibiotics to control infections (Lewis,

2020). To combat AMR this time, an overall holistic approach comprising proper surveillance, antibiotic detoxification system development- wastewater treatment (Li *et al*., 2022) as well as antibiotic stewardship (Carrara *et al*., 2024) seems essential.

1.3 HYPOTHESIS

1.3.1 Null Hypothesis:

Antibiotics and biogenic silver nanoparticles could not be produced by the isolated *Streptomyces* from the Illam soil sample.

Potential lead molecules will not be screened against the resistant elements Cfr.

1.3.2 Alternate Hypothesis:

Antibiotics and biogenic silver nanoparticles could be produced by the isolated *Streptomyces* from the Illam soil sample.

Potential lead molecules will be screened against the resistant elements Cfr.

1.4 OBJECTIVE

1.4.1 General objective

To study the potential of antibiotic and Biogenic AgNP synthesized from *Streptomyces* with in silico potentiator screening against resistant element Cfr.

1.4.2 Specific objectives

- To isolate and characterize *Streptomyces sps*. and AgNP.
- To test the efficacy of antibiotic and biogenic AgNP from *Streptomyces sps*.
- To extract, prepare, dock and screen potential Cfr potentiators by in silico.

1.5 RATIONALE

This study focuses on the identification of potentiators to render effectiveness of PhLOPS drugs against resistant element Cfr.

1.6 SCOPE

The present study focuses on identifying potential lead molecules among the natural product compounds against Cfr target in emerging multidrug resistant pathogen *Staphylococcus aureus*. Furthermore, robust screening and antimicrobial assays have been sought with other alternatives to antibiotics such as silver nanoparticles for antimicrobial properties, function and effectiveness.

2. LITERATURE REVIEW

2.1 Antibiotic history

Although the antibiotic was officially discovered in 1928 for the first time, their reported use dates back well over 2,500 years ago to ancient Chinese. Other ancient civilizations (ancient Egyptians and ancient Greeks) also used molds and plants to treat infections without knowing the actual compound responsible for developing antibiotic action (Kourkouta *et al*., 2018). From that ancient period to the present day, the scope of discovering new antibiotics looks only slimmer, with no new class of antibiotic discovery taking place. The last time a new class of antibiotic discovered was daptomycin and linezolid in 1980 (Durand *et al*., 2019).

2.1.1 Antibiotic producers

The list of antibiotic producers includes fungus and soil bacteria; however, plant also joins the ally as they are source of wide variety of secondary metabolites (tannins, terpenoids, alkaloids, and flavonoids) with antimicrobial properties (Cowan, 1999). Among the soil dwelling bacteria, the *Actinomycetes* dominates the chart for producing most of the existing arsenal of antibiotics. In recent times, the *Actinomycetes* has established itself as a group of dynamic and diverse organisms with utilities in various sectors like pharmaceuticals, agriculture and biofortification, bioremediation, nanotechnology and enzyme industries. However, it is distinctly known for its ability to produce valuable pharmaceutical metabolites such as antibiotics, antifungals, anticancer and anti-inflammatory molecules (Oli *et al*., 2021). In addition, since these organisms thrive in saprophytic environment and places where the complex organic matter is affluent, they are equally explored for its ability to produce industrially important enzymes such as amylase, chitinase, keratinase, cellulase, lignocellulolytic enzymes and more. Furthermore, due to close association with plant and forest ecosystems associated with trees as well, it is explored for agricultural symbiotic defense research for crop improvement and agricultural product development such as bio pesticides. Moreover, currently, human gut microbiota is also becoming a new exploration area in antibiotic discovery with many identified biosynthetic gene clusters (Durand *et al*., 2019).

The *Actinomycetes* are a group of gram-positive bacteria belonging to the order *Actinomycetales* of the phylum *Actinobacteria* with high guanine (G) and cytosine (C) content in their DNA. They are a large and diverse group in the bacterial domain, with at least 350 genera known to date. They constitute one of the largest bacterial phyla prevalent in aquatic as well as terrestrial ecosystems (Takahashi & Nakashima, 2018). *Streptomyces, Norcardia, Micromonospora* are the major genus dominating the order

along with other genus including *Actinomyces, Rhodococcus, Nocardioides,* and *Pseudonocardia*. The *Actinomycetes* has been recognized as prolific producers of enzymes, antibiotics, anticancer agents for the longest time and for playing a major role in recycling of organic matter in nature (Lee *et al*., 2020).

2.1.2 Genus: *Streptomyces*

The superior genus in the group of *Actinomycetes* is *Streptomyces* accounting for more than 95% of all *Actinomycete* strains isolated from soil (Williams & Vickers, 1988). *Streptomyces* are filamentous, spore-forming, aerobic, non-acid-fast bacteria characterized by an earthy-musty odor, reminiscent of freshly turned soil (Liato & Aïder, 2017). They have been successful in yielding a vast number of antimicrobials for decades now. Furthermore, it has been revealed from a whole-genome sequence analysis of *Streptomyces coelicolor*, a representative of the genus *Streptomyces* that their genome encoded the potential to synthesize 10-fold the number of antibiotics currently being produced. However, those antibiotic-synthesis clusters are not expressed usually but found to be triggered by stress or extreme environmental conditions, referring to them as 'Silent Clusters' (Chiang *et al*., 2011). Therefore, extreme environments or environments that promote secondary metabolite production have been a go-to area for collecting soil samples in the hopes to discover *Streptomyces* expressing different collections of antibiotics (Quinn *et al*., 2020).

2.1.3 Bioactive secondary metabolite production

Though not essential for organisms' viability, secondary metabolites are the bioactive compounds that offer a competitive edge in continuing its survival among other organisms in their environment. Hence the compounds that are not principal molecules for organisms' survival but play a crucial role in ensuring their survivability (such as antibiotic, toxins, antifungal, antiviral, alkaloids, essential oils and more) in their natural habitat are simply known as secondary metabolites. Due to a sedentary and sessile lifestyle, nature seems to have equipped these organisms with this ability to defend themselves and continue its existence in the ecosystem. In different phases and stages of life these molecules are produced by plants and microorganisms, however, *Streptomyces* produce these compounds in stationary phase when it is not required for growth but provides competitive supremacy over other organisms in their niche (Alam *et al*., 2022). On the contrary, these secondary metabolites are produced in limited amounts and are dispersed in broth, which is why it further needs to be concentrated before its efficacy can be tested. Since they are organic molecules, various organic solvents are employed for metabolite extraction based on their polarity (Roopashree & Naik, 2019). The solvent often used in antibiotic extractions are: Butanol and ethyl acetate (Ilić *et al*., 2007; Sah *et al*., 2021).

2.1.4 Biogenic AgNP synthesis

Nanotechnology is one of many rapidly emerging branches of science due to diverse applications of nanomaterials in material science, medical sciences and biology (Kesharwani *et al*., 2018). It deals with nanomaterials (sizes in nanoscales 1 nm to 100nm), its characterization, designing, and application in the real world. One of the most researched nanoparticles is of Silver origin. Silver nanoparticle is made up of 20 to 15,000 silver atoms, its diameter ranging within the nanoscale, 100 nm. Silver nanoparticles are known to show remarkable antimicrobial activity even at a low concentration due to large surface area-to-volume ratio (Oves *et al*., 2018).

Biologically, silver nanoparticles have been reported to be synthesized using plant extracts as well as microbial extracts from fungus and *Streptomyces*. The biogenic AgNP synthesis approach also known as green synthesis has emerged as a sustainable process to overcome limitations of physicochemical methods. The Biogenic AgNP synthesis not only limits the usage of toxic reducing agents but also prevents adoption of physical methods of AgNP synthesis employing hazardous radiation that release toxic byproducts. It also exhibits eco-friendly property offering high stability, with less complex procedure and cost-effectivity (Parveen *et al*., 2016).

The application of AgNP in the field of agriculture and healthcare as growth promoter in crops, wound treatment, drug delivery, medical imaging, molecular diagnostics, joint replacement fabrication, anticancer and nano drugs formulation as well as biosensors (H_2S), has increased its demand. Apart from that, AgNPs has also been known for its antibacterial efficacy against emerging pathogenic bacteria hence, is relevant for this study. Despite the obscure mechanism of antibacterial action of silver nanoparticles, the mechanism such as destruction of cell wall, plasma membrane, cytosolic proteins and enzymes are some of the proposed ones to be responsible for its antibacterial activity. Regarding silver nanoparticles, the proposed antibacterial actions are continual release of silver ions killing microbes (Bapat *et al*., 2018), adherence to cell wall and cytoplasmic membrane enhancing permeability leading to bacterial cell disruption (Khorrami *et al*., 2018), deactivation of respiratory enzymes, ROS generation and interruption of ATP production; interaction with sulfur and phosphorus components of DNA resulting hindrance in DNA replication and cell reproduction; ribosome denaturation (Durán *et al*., 2016) and more (Yin *et al*., 2020). Recent research has reported biogenically synthesized AgNP from *Streptomyces sps* extract demonstrating better inhibition to meningitis-causing bacteria compared to their secondary metabolite counterparts (Bano *et al*., 2023). Therefore, we explore the genus of *Streptomyces* for biogenic AgNP synthesis for antimicrobial activity assessment in this research.

2.2 Target modification: An antimicrobial resistance mechanism

The *Cfr* gene in methicillin-resistant *Staphylococcus aureus* (MRSA) is an example of target modification antibiotic resistance mechanism found rendering eight important classes of antibiotics: phenicols, lincosamides, oxazolidinones, pleuromutilins, and streptogramin A antibiotics (Long *et al*., 2006); nucleoside analog A201A, hygromycin A (Polikanov *et al*., 2015) and 16-membered macrolides (Smith & Mankin, 2008), ineffective to treat the infection including the synthetic antibiotic class of oxazolidinone-Linezolid, referred as the last line of defense in MRSA infection treatment. Clinical pipeline of antimicrobial compounds indicates that in last couple decades, lipopeptides (daptomycin) and oxazolidinones (Linezolid) are the only new class of antimicrobials that has been approved for clinical use (Mendes *et al*., 2014). This oxazolidinone drug has inhibitory activity against essentially all Gram-positive organisms, including methicillin-resistant *Staphylococcus aureus* (MRSA), vancomycin-resistant *Enterococci* (VRE) (Mendes *et al*., 2014) and penicillin-resistant *Pneumococci*, which now has become ineffective as a consequence of target modification by resistant element Cfr.

2.2.1 Cfr as a target

Among different classes of antibiotics, a significant number of antibiotics are available that cease viability of bacteria by targeting and binding to rRNA of the important protein synthesizing machinery, the ribosome of the cell (Arenz & Wilson, 2016). Similarly, bacteria also have developed resistant mechanism to counter it by altering its genetics, developing rRNA methylating enzyme encoding chloramphenicol-florfenicol resistance (*Cfr*) and *RlmN* genes known for inserting a small modification into the ribosome that alter antibiotic binding pockets and prevents antibiotics from binding to it. As a consequence, the antibiotics cannot inhibit protein synthesis making them ineffective against the infection (Tsai *et al*., 2022). Cfr and its homolog RlmN are two radical SAM enzymes that methylate and modify (C8 and C2 amidine carbon of adenosine respectively at 2503 of 23S ribosomal RNA in peptidyl transferase center) the ribosome as an antibiotic target.

The first case of resistant mechanism from *Cfr* was documented in 2007 in *Staphylococcus aureus* isolate (Arias *et al*., 2008) derived from patient and subsequently, it has been identified in various gram positive as well as gram negative bacteria resulting in severe antibiotic resistance outbreaks to oxazolidinone- linezolid (Dortet *et al*., 2017), one of the last-resort synthetic antibiotic (Dembicka *et al*., 2021) used to treat gram-positive bacterial infections in clinical setup. Since then, the *Cfr* gene has also been identified in the veterinary isolate of *Staphylococci* and reported present on plasmids indicating the potential horizontal transfer of the resistance within the genera (Kehrenberg *et al*., 2007). Therefore, the solution to this is absolutely essential

which is why Cfr has been explored as a potential target in this study.

2.2.2 Antimicrobial Potentiator

The concept of antimicrobial potentiator is not new. In fact, it has been a part of therapy for decades now. As aforementioned, several strategies have advent along the journey of new antibiotic discovery, such as active uptake pathways hijack, potentiator approach, bacterial virulence factor blocking and more in antibiotic domain (Baker *et al*., 2018). One of such strategies is antibiotic resistance reversal, also known as potentiator approach, principally directed towards antibiotic resistance mechanisms that effectively potentiates antimicrobial action. These kinds of compounds which do not have an inherent antimicrobial activity of its own (Moo *et al*., 2020) but equips respective antibiotics to retain its mode of action are called resistance breaker or antibiotic potentiators or adjuvants (Chawla *et al*., 2022). Hence, strategies like discovery of enzyme inhibitors have been developed to restore the utility of such antibiotics. The potentiators serve purposes such as antimicrobial resistance element inhibition, antimicrobial uptake enhancement in targeted cells, nullifying effects of efflux pump, biofilm disruption and boost/foster oxidative stress in bacteria. The various examples of antimicrobial potentiators are already available in use, for instance, the Clavulanic acid and tazobactam has been in use in combination with amoxicillin and piperacillin, respectively for serine β-Lactamases (SBLs) resistance element inhibition (Lewis, 2020). In addition, an active compound angucyclinones 8-*O*-methyltetrangomycin (MTN) and 8-*O*-methyltetrangulol (MTL) from in-house library of microbial (*Streptomyces sps*) natural product extract has been reported to potentiate $PhLOPS_A$ (Schaenzer *et al*., 2023). Furthermore, in a recent study, in silico virtual screening has shown promising results in identifying an effective, new meropenem potentiator that has shown activity against carbapenemase-producing *Enterobacterales* (Zheng *et al*., 2024), hence a similar approach is adopted in this research to screen the PhLOPS potentiators against the target Cfr employing the computational molecular docking tools.

2.3 Computer Aided Drug Designing

The process of adopting computer and computational approaches for discovery, development, and assessment of molecules and compounds for its bioactive property and potential is called Computer Aided Drug Designing (CADD) (A. Kumar & Jha, 2017). CADD is highly accurate and efficient. It can take a large number of molecules in batches and screen them through a set of algorithms to assess the suitability of the ligands by orienting the compounds in various configurations and considers different factors such as presence of functional groups in the compound its nature and interaction with amino acids residues in the target along with the analysis of hydrophobic interactions for target-ligand interactions. Apart from screening of drug like entities, CADD is equally

useful in predicting and modeling 3D structure of unknown targets, compound searching based on similarity, target identification, binding site prediction, protein-ligand binding dynamic analysis, predicting ADMET properties, biological activity and more (Tiwari & Singh, 2022).

2.3.1 Virtual Screening of potentiators with druggable Properties

While high-throughput screening (HTS) is a process of actually screening the library of real compounds available in laboratory against a selected target, virtual screening is the same process which occurs in a computer system where large library of compounds from databases are obtained and screened against the target also obtained from database in a screening specific computational programs and software (Gimeno *et al*., 2019). This process offers us with valuable insights and indicative parameters for selection of compounds to actually conduct experiments in real laboratories and assess its viability, saving a lot of time and resources. It has led us to rationalized decision making in drug discovery rather than random hit and trial. Recently, virtual screening has been utilized for diverse purposes such as lead identification, lead optimization and scaffold hopping (Zheng *et al*., 2021) as it is a quick and budget-friendly method.

The virtual screening is of two types, ligand based virtual screening (LBVS) and structure based virtual screening (SBVS). In LBVS, ligands known to bind a specific target are used as a template for identifying similar compounds from a pool of ligand virtual databases. This method is much faster than SBVS and can be performed in standard CPU, used when the specific target is unknown or X-ray structure of the target is unavailable. On the other hand, Structure based approach also known as docking method is opted if the 3D structural information of the target is known (Tôrres *et al*., 2019). In comparison to LBVS, it is highly resource demanding and time consuming as heavy algorithms are assigned and performed to solve the task and it also requires high computational power. Hence, in this study, we will be focusing on SBVS against the target Cfr whose homolog RlmN is known. The general method of structure based virtual screening includes the steps: target identification, 3D structure obtaining or model building and validation, identification of active sites, ligand library selection, protein and ligand preparation, library design, docking, target-ligand interaction analysis and more.

2.3.2 Molecular Docking

Molecular docking is a powerful computational tool in structural molecular biology used to design drugs, predict the binding affinity and analyze how ligands interact with the receptor (Fan *et al*., 2019). With the availability of sizable experimental data of protein structure from X-ray crystallography and nuclear magnetic resonance (NMR), molecular docking has become an extensional tool in drug discovery. The molecular docking functions by a set of algorithms designed to search and evaluate conformation of

compounds in high-dimensional spaces recursively until it attains the minimum energy. Then, an affinity scoring function, ΔG [U total in kcal/mol], is employed to rank the candidate poses as the sum of the electrostatic and van der Waals energies. Hence, it can be used to conduct virtual screening on large libraries of ligands, rank the results further using the insights for structural hypothesis proposition of target inhibition for lead optimization (Morris & Lim-Wilby, 2008). Now that docking against homology-modeled targets of proteins whose structures are unknown has also become possible, it has become even more valuable (Pagadala *et al*., 2017). This tool is highly efficient and low on research cost. In addition, reverse molecular docking technology is another aspect that capacitates with improved drug target prediction (Fan *et al*., 2019). However, the results obtained by molecular docking solely cannot be concluded as accurate unless it is tested and confirmed by other thermodynamics featured techniques like Molecular dynamic simulation and further wet lab verification for its actual efficacy.

3. MATERIALS AND METHODS

3.1 Materials, reagents and chemicals used in the study

The test organisms *Klebsiella pneumoniae* 700603, *Escherichia coli* 25922, *Staphylococcus aureus* 29213 used in this study were available at Central Department of Biotechnology, Tribhuvan University. Other chemicals were obtained from commercial suppliers, Himedia and Merck and Thermo- Fisher company.

3.2 Secondary metabolite antibacterial efficacy testing

3.2.1 Selection of soil samples and sample collection

The soil samples were collected from Goruwale Bhanjang in Ilam district of eastern Nepal. The area was chosen for sampling because it is home to Himalayan endemic plants with potential to produce a larger number of secondary metabolites than any other region in Nepal. Furthermore, the district covers the tropical to alpine range of vegetation (DDC,2015) and the climate of Ilam is considered to induce secondary metabolite producing potential in plants as the factor of elevation has been reported to affect the amount of secondary metabolite production in plants (Zargoosh *et al*., 2019). Moreover, a cytological study by Schinkel indicated polyploidy in plants being related to cold tolerance and robustness as an adaptation to conditions at high elevation with fitness advantage, hence hoping to isolate more robust *Streptomyces sps.* from the area, the selection of this location was done. The soil samples were collected from 9 different sites in Ilam.

The detailed information of the sites of sample collection is presented in the table below.

Table 1: Sample collection area

Samples	Geographic position	Elevation from sea level
BG01	**27°6'4''N 87°55'28''E**	**2840.6m 9211ft**
BG02	**27°6'1''N 87°55'33''E**	**2837.5m 9201ft**
BG03	**27°5'56''N 87°55'49''E**	**2836.4m 9197ft**
BG04	**27°5'59''N 87°55'57''E**	**2791.4m 8818ft**
BG05	**27°5'59''N 87°55'57''E**	**2730.7m 8854ft**
BG06	**27°5'58''N 87°55'57''E**	**2735.2m 8869ft**
BG07	**27°3'39''N 87°56'26''E**	**2735.7m 8871ft**
BG08	**27°5'59''N 87°55'59''E**	**2739.3m 8882ft**
BG09	**27°5'59''N 87°55'59''E**	**2739.1m 8882ft**

3.2.2 Soil treatment, media selection and Primary culture

0.1gm of each soil sample were weighed then dissolved in 900 µl sterile autoclaved water followed by moist heat treatment at 80^0C (water bath) for 10 minutes. Then the initially diluted samples were diluted further up to dilution factor of 10^{-5}, spread plated in

respective modified media plates and left for incubation for 7 to 15 days at 28-30^{0}C. Similarly, the modified media containing tannic acid incorporated with indole butyric acid and tryptophan respectively (developed in previous projects (Sita Ghimire, M. Sc. Thesis, 2019)), was employed in this research to screen potential *Streptomyces sps*. The modified media compositions are as follows.

Table 2: Modified media composition

S. no.	Components	gm/L
1	Tannic acid	0.025
2	Ammonium sulphate- $(NH_4)_2SO_4$	1
3	Dipotassium Hydrogen Phosphate- K_2HPO_4	0.8
4	Potassium Dihydrogen Phosphate- KH_2PO_4	0.2
5	Magnesium sulphate- $MgSO_4.7H_2O$	0.5
6	Calcium sulphate- $CaSO_4.7H_2O$	0.05
7	Mineral mix	10
8	Vitamin mix	10
10	Indole butyric acid or tryptophan	0.025

Table 3: Mineral mix composition

S. no.	Components	gm/L
1	Potash Alum (Aluminium potassium sulphate)	0.01
2	Boric acid	0.01
3	Calcium Chloride	0.1
4	Cobalt Chloride	0.1
5	Cobalt nitrate hexahydrate	0.2
6	Manganese Sulphate	0.5
7	Sodium Chloride	1
8	Sodium Molybdate	0.025
9	Sodium Tungstate	0.025
10	Zinc Chloride	0.13

Table 4: Vitamin mix composition

S. no.	Components	mg/L
1	Biotin	2
2	Folic acid	2
3	Pyridoxine	10
4	Thiamine	5
5	Nicotinic acid	5
6	Pantothenic acid	5
7	Vitamin B12	0.1
8	P-Aminobenzoic acid	5
9	Sodium Tungstate	0.025

3.2.3 Macroscopic colony study and pure culture isolation

The colony characteristics of *Actinomycetes* and *Streptomyces* such as dry, chalky, powdery, colonies arranged in concentric fashion features of colonies were looked for to proceed ahead the isolation in starch casein agar (SCA) plate for further pure culture

isolation.

3.2.4 Colony identification by Morphology and Gram staining

The colony morphology of the isolates was noted and then the gram staining was performed to identify isolates as gram positive filamentous bacteria. Firstly, the smear of respective isolates was prepared, heat fixed and stained with crystal violet (primary stain) for one minute and water rinsed, followed by fixing with gram's iodine for another one minute and water rinsing. Then the decolorizer is applied for 20-30 seconds and rinsed following counter-staining with safranin for one minute and rinsing. Finally, the slides were then left for air dry. The slides were then observed under microscope at 40X and 100X magnification to identify the isolates as gram positive filamentous bacteria.

3.2.5 Enzymatic Assay

Additionally, enzymatic assay was conducted to characterize biochemical properties of the isolates. The enzymatic assay comprised of Starch hydrolysis, Gelatin hydrolysis, Cellulose enzymatic assay, Nitrate Utilization and 13 (Melibiose, Sucrose, Erythritol, Xylose, Sorbitol, Maltose, Galactose, Inositol, Ribose, Mannitol, Lactose, Fructose, and Glucose) different carbohydrate utilization.

3.2.5.1 Starch Hydrolysis test

For the Starch hydrolysis test, nutrient agar plates containing 1% starch were prepared then the isolates were cultured by streaking. The plates were then incubated at 28-30 ^{0}C until growth of the isolates were observed. The plates were then subjected to iodine solution followed by de-staining with NaCl to visualize the zone of starch hydrolysis.

3.2.5.2 Cellulose Hydrolysis test

The 1% cellulose incorporated nutrient agar plates were prepared, in which the respective isolates were streak cultured. The plates were then incubated at 28-30 ^{0}C until growth of the isolates were observed. The plates were then subjected to 1% congo red solution followed by 15 minute of plate shaking to visualize the zone of cellulose hydrolysis.

3.2.5.3 Gelatin Hydrolysis test

The 1% gelatin incorporated nutrient agar plates were prepared, in which the respective isolates were streak cultured. The plates were then incubated at 28-30 ^{0}C until growth of the isolates were observed. Few drops of acidic $HgCl_2$ reagent was then added to the plates in order to visualize the zone of gelatin hydrolysis.

3.2.5.4 Carbohydrate Utilization test

Carbohydrate fermentation protocol by Karen Reiner, 2012 (American Society for Microbiology) was employed for this test. The respective carbohydrate (0.5-1%) and indicator (Phenol red) incorporated peptone water broths (in distilled neutral pH water)

were prepared and transferred in test-tubes followed by introduction of Durham's tube and autoclaved. Then, aseptically, each isolate was inoculated in respectively labeled broths and incubated for 18 to 24 hours. The broths were then observed for color change from red to yellow for positive carbohydrate utilization test and the results were recorded.

3.2.5.5 Nitrate Reduction test

Nitrate Broth was prepared and transferred in clean culture tubes and autoclaved. A pure colony of the potential *Streptomyces* isolates were inoculated aseptically in each tube. The tubes were then incubated at 30^0C for 48 hours. After that, 5 drops of nitrate solution A and B were added and red coloration was observed. If necessary, a pinch of zinc powder was added and looked for the development of red color.

3.2.6 Primary screening against ATCC test pathogens

Different American Type Culture Collection (ATCC) bacteria named as *Klebsiella pneumoniae* 700603, *Escherichia coli* 25922, *Staphylococcus aureus* 29213 were obtained from Central Department of Biotechnology (CDBT) laboratory and isolated from glycerol stock in Nutrient broth agar plates. The Muller Hilton Agar (MHA) plates were prepared and the potential *Streptomyces* isolates were streaked perpendicularly at the center of the plate and incubated for 5-7 days at 28 to 30^0C. After that, the test organisms were horizontally streaked perpendicularly to the isolate streaking and incubated at 37^0C for 18 to 24 hours. The plates were then observed for lines of inhibition.

3.2.7 Secondary metabolite production

For the secondary metabolite production, two different media were prepared for antibiotic extraction (ISP4) and silver nanoparticle (Starch casein broth). The media compositions are as follows:

Table 5: ISP4 broth composition

Components	gm/L
Soluble starch	10
Magnesium Sulphate- $MgSO_4 . 7 H_2O$	1
NaCl	1
Ammonium Sulphate- $(NH_4)_2. SO_4$	2
Calcium carbonate- $CaCO_3$	2
trace salt solution: 0.1g Ferrous sulphate- $FeSO_4.7 H_2O$ 0.1g Manganese chloride- $MnCl_2. 4H_2O$ 0.1g Zinc sulphate- $ZnSO_4. 7 H_2O$ In 100ml	1 ml
pH	7 to 7.4

Table 6: Starch Casein Broth composition

Components	gm/L
Soluble starch	10
Casein (vitamin free)	0.3
KNO_3	2
Magnesium Sulphate- $MgSO_4 . 7 H_2O$	0.05
K_2HPO_4	2
NaCl	2
Ferrous sulphate- $FeSO_4.7 H_2O$	0.01
Calcium carbonate- $CaCO_3$	0.02
pH	7.0 ± 0.1

3.2.7.1 Antibiotic extraction

The active isolates were cultured on respective ISP4 broth for 7-15 days at 28-30 ^{0}C in a shaking incubator, followed by centrifugation at 4100 rpm and filtration of the solution. Subsequently, each filtrate was subjected to ethyl acetate solvent-metabolite extraction method by mixing equal volume (1:1) of filtrate broth and the ethyl acetate (Ilić *et al*., 2007; Sah *et al*., 2021). The mixture was then left overnight for shaking followed by separation of ethyl acetate layer from the aqueous layer using a separating funnel. The ethyl acetate layer was then collected and concentrated in a rotary evaporator. The extract was then collected in Eppendorf tubes, allowed to dry and finally stored in the refrigerator for later use.

Figure 1: Separating funnel **Figure 2: Antibiotic concentration in rotary evaporator**

3.2.7.2 Antimicrobial susceptibility plate assay

The test pathogen broth cultures were adjusted to 0.5 McFarland equivalent or an absorbance of 0.08 to 0.1 at 600nm. Meanwhile, Mueller Hinton agar plates were prepared, punched holes by the help of borer and a swab of McFarland test cultures were carpet cultured in MHA plate. Finally, the various extracts (50 mg/ml) prepared by dissolving the dry extract in 100% and 50% dimethyl sulfoxide (DMSO) respectively were

placed (20µl) in the respective hole for inhibition.

3.2.7.3 Resazurin antimicrobial assay for MIC MBC determination

The resazurin based microdilution antimicrobial assay method was employed for determination of MIC and MBC of respective antimicrobials (I53 secondary metabolite extract and I53 AgNP) against test organisms as devised in a protocol by Elshikh *et al*., 2016. Prior to the actual experiment, the performance of standard antibiotics Tetracycline and chloramphenicol was tested against ATCC strains for standardization with the MIC MBC values in the Clinical and Laboratory Standards Institute (CLSI).

14 times serial double dilution was performed starting with the concentration of 2mg/ml to 0.0001220703125mg/ml or 0.122µg/ml.

The initial concentration of 63.33mg/ml of I53 antibiotic extract was taken and serial double dilution was done 9 times up to 3.8µg/ml. Similarly, initial concentration of 3.33mg/ml Silver nanoparticle was prepared and serial diluted 19 times up to 0.0123.8µg/ml by double dilution.

Similarly, the respective stock solution of the antimicrobials (antibiotic and AgNP) was prepared by dissolving it in 50% DMSO and sterile water respectively. A series of epi tubes were labelled and 50µl MHB was dispensed in the respective tubes, to which, double serial dilution was performed by transferring 50µl of stock antimicrobials to subsequent epi tubes. Now, the standard McFarland test suspension was diluted by 1:100 in MHB broth and 50µl of the diluted test suspension was added to double serial dilution antimicrobial suspension making the final volume of 100 µl. Similarly, in three separate epitubes, 100µl of diluted suspension of each test organism (*Klebsiella pneumoniae* 700603, *Escherichia coli* 25922, *Staphylococcus aureus* 29213) was dispensed for positive control. In one epitube, 100µl MHB only was dispensed for broth sterility testing. The tubes were then incubated for 24 hours at 37^0C. Finally, followed by proper incubation, 20µl of resazurin (0.15mg/ml) (Riss *et al*. 2016) was added and further incubated for 2-4 hours for color change due to the conversion of resazurin to resorufin as a result of an active bacterial metabolism. The color change was observed for MIC determination and further for MBC, the tubes retaining purple color of resazurin were plated in Nutrient agar plates and incubated for 24 hours at 37^0C for observation of test organism growth. Same procedure was followed for AgNP MIC-MBC determination where AgNP was washed with 70% ethanol followed by its stock preparation in sterile water. All the experiments were conducted in triplicates.

3.2.8 Molecular characterization of isolate

For molecular characterization of the isolate, genomic DNA was extracted for which, the isolated colony of potential isolate was cultured in 10ml ISP2 broth. The DNA extraction was then carried out manually by salting out genomic DNA Extraction method -ActinoBase

(Kieser *et al*. 2000) with slight modification. First, the culture broth was centrifuged for pellet collection which was then suspended in a 5ml SET buffer in a 50 ml falcon. To it, 100µl lysozyme was added and incubated for 1 to 3 hours at 37^0C. The completion of the lysis is indicated when reaction became clarified and turned viscous. Now, 140µl proteinase K and 600µl 10% SDS was added and mixed by inversion followed by incubation at 55^0C for 2hrs with occasional inversion. Then 2 ml 5M NaCl was added to it, mixed by inversion and allowed to cool at room temperature. After that, 5ml chloroform was added to it, mixed by inversion for 30 mins at room temperature and finally centrifuged at 4200 rpm for 15 mins. After centrifugation, the top clear layer was carefully collected in a clean tube and incubated on ice for 2mins, then added 0.6 volume ice cold isopropanol. It was then mixed by inversion and further incubated on ice for 3-5mins. It was then transferred in a spin column, centrifuged at 12,000 rpm for 30 sec and the flow through was discarded. The spin column was then washed with 70% ethanol 2-3 times, centrifuged at 12,000rpm for 2 mins and left to air dry for 3-5mins. Then, 20 to 50µl TE buffer was placed in the center of the spin column, incubated at room temperature for 10 to 15 mins and then collected in a new sterile epitube. The gDNA was then run with Solis biodyne, a 100bp ladder in 1% agarose gel electrophoresis and visualized in Gel-Doc.

3.2.8.1 16S rRNA amplification

The extracted DNA was subjected to following conditions with compositions mentioned as follows for 16S rRNA amplification. The PCR product was then run in 1% agarose gel electrophoresis and visualized in Gel-Doc.

Table 7: PCR Mixture Compositions

Components	µl
Water	0
2X Kapa	12.5
16sBakt341F (1pmol/ul)	**5**
16sBakt805R (1pmol/ul)	**5**
Template	**2.5**
Total	**25**

Table 8: PCR Conditions

Temperature	**Time**	Cycles
95^0C	3 min	1
98^0C	30 s	35
65^0C	25 s	
72^0C	20 s	
72^0C	5 min	1
4^0C	HOLD	1

3.2.8.2 Sequencing, alignment and phylogenetic tree construction

The 16s rRNA product was sent for sanger sequencing and the obtained sequence was then performed BLAST in the website of NCBI. The different organism's sequence obtained from the aligned results were selected and further used to construct a phylogenetic tree in MEGA11 evolutionary genetics analysis software using the method of maximum likelihood. Prior to subjecting the sequences to method of maximum likelihood, the system was setup for finding a best model and hence T92 (Tamura-3-parameter) model was employed to carry out the maximum likelihood phylogenetic analysis.

3.3 Antibacterial efficacy testing of biogenic AgNP

3.3.1 Silver nanoparticle synthesis

Biogenic AgNP was synthesized by employing the protocol as mentioned/described in the research paper by Wypij *et al*. (2018); Sambangi, P., & Gopalakrishnan, S. (2023). The isolate culture broth (Starch Casein Broth) was centrifuged, filtered and then mixed with equal volume of $AgNO_3$ (10mM). The final pH of the mixture was adjusted to alkaline 8.5. Then it was left at room temperature for 5-8 days and observed for reddish-brown color development of silver nanoparticles.

3.3.2 UV-Vis spectrophotometer analysis

The silver nanoparticle formation was observed for color change, then the solution was subjected to UV-Vis spectrometry for absorbance spectrum analysis in the 300-700 nm wavelength range. For this, the sterile water was taken as reference. The UV–visible spectroscopy was measured in a quartz cuvette using a 1 nm resolution Shimadzu dual-beam spectrophotometer (model UV-1800). Visualizations of the samples' measured optical densities (O.D.) were then analyzed. The data obtained was then plotted in a graphical form and the maximum absorbance wavelength was determined using Origin 2023b SR1 software.

3.3.3 AgNP FTIR characterization

To estimate the functional groups on the NP's surface, FTIR assay is used, hence to examine FTIR pattern of protein interaction with NPs, the NP in suspension was centrifuged at 5000-10,000 rpm for 20-30 min, the pellets were then washed several times, dried, and the powder was examined using FTIR at 400–4000 cm^{-1}. The purpose of FTIR is to analyze how the sample absorbs much light at each wavelength. The obtained data was then fed in the Origin software to generate the transmittance-wavenumber graph.

3.3.4 Resazurin antimicrobial assay for MIC MBC determination

Same resazurin microdilution protocol as used for antibiotic efficiency determination was employed for MIC MBC determination of biogenically synthesized AgNP.

3.4 In Silico potentiator screening against Cfr

3.4.1 Target selection

First of all, through literature review the AMR resistant target element Cfr and RlmN was identified for potentiator screening.

3.4.1.1 3D crystal structure search and building

The 3D structure and active sites of respective targets Cfr and RlmN was sought in the rcsb data bank. The RlmN crystal structure was obtained from the rcsb database with **PDBID:**

3RFA. The 3D structure of Cfr and its active site was not available in the database of rcsb, hence its 3D structure was constructed using Alphafold (Jumper *et al*., 2021) (sequence derived from NCBI. **Accession no. AMN16502.1**). Prior to that, sequence alignment of Cfr protein was done with RlmN using the BLAST tool in NCBI. For the active site prediction, the multiple sequence alignment was performed using Clustal Omega and the residues aligning with active site residue of 3RFA was considered for docking. Furthermore, the 3D structure of Cfr and its homolog RlmN was also aligned and visualized in Pymol to analyze its structure similarity.

3.4.1.2 Target 3D structure validation

The targets RlmN and Cfr were validated by Z-score and Ramachandran plot analysis using proSA web server and SAVES V 6.0 web server respectively.

3.4.1.3 Protein preparation

Prior to conducting molecular docking, both the protein and ligands need to be prepared, hence, it was achieved by using tools such as Pymol and Autodock. The protein was prepared by a series of steps: removing water molecules, adding hydrogen atoms, merging non-polar bonds, adding gasteiger charges, removal of native ligand if present and finally saving and converting it to pdb and pdbqt format respectively.

3.4.2 Ligand library Preparation

For ligand library preparation, the natural compound library was extracted from Zinc15.org and pubchem. Furthermore, its native ligand SAM and SAH was also obtained for future screening procedures.

3.4.2.1 ADME/TOX filter

The extracted compounds were subjected to the ADMET filter which stands for Absorption, Distribution, Metabolism, Excretion and Toxicity. The OSIRIS-DataWarrior (Sander *et al*., 2015) was used to screen the ligands based on toxic profiles and drug-likeness based on parameters such as molecular weight, cLogP, cLogS, druglikeness, total polar surface, rotatable bonds and toxicity (mutagenicity, tumorigenicity, reproductive effects and irritant effects). The parameters for filtering ligands based on drug-likeness are as follows:

Table 9: ADME/Tox Filter

Parameters	Filter range
Molecular weight	200 to 500 Daltons
cLogP	-3 to 6
cLogS	-4 to -2
Hydrogen bond donors	0 to 5
H-bond acceptor	0 to 10 (Lipinski *et al*., 1997)
TPSA	0 to 120
Rotatable bonds	10 or less (Veber *et al*., 2002)
Druglikeness	positive value
Mutagenic	None
Teratogenic	None
Tumorogenic	None
Irritant none	None
Reproductive effect	None

3.4.2.2 Protein and ligand library preparation in dockable format

The ligands were prepared in bulk using Openbabel GUI (O'Boyle *et al*., 2011), an available feature in PyRx 0.9.8 setup adopting forcefield energy minimization and subsequent bulk conversion to pdbqt, a dockable file format.

3.4.3 Molecular Docking

The structure based virtual screening was carried out employing a molecular docking tool PyRx 0.9.8 against the filters HMAT1A, Cyp3A4 and target proteins Cfr.

3.4.3.1 Filter 1: Docking against HMAT1A protein

hMAT1A stands for human methionine adenosyltransferase expressed in the liver that catalyzes the synthesis of S-adenosylmethionine, a major biological methyl donor, critical for drug metabolism, hepatic health and immune modulation. It plays a crucial role in methyl conjugation of drugs, xenobiotics, hormones, neurotransmitters as well as DNA, RNA and proteins (Mato *et al.*, 1997). Furthermore, it plays a major role in critical pathways such as transmethylation (in immunity and cell signaling) (Lawson *et al*., 2012), trans-sulfuration (cysteine and glutathione- essential non-enzymatic antioxidant, synthesis pathway) (Pérez-Sala *et al*., 2018), and polyamine synthesis (Park & Igarashi, 2013). Therefore, prior to docking the ligand library with the target Cfr, docking of ligand library was performed with hMAT1A **(PDBID:6SW5)** and further the screened ligands having lower binding energy with respect to its native ligands SAM and SAH were screened and sorted for further screening procedures.

3.4.3.2 Filter 2: Docking against human cytochrome p450 Cyp3A4 protein

The cytochrome P450 enzymes are crucially essential for drug response (Guengerich, 2022), catalyzing a wide range of reactions associated with metabolic reactions of xenobiotics (drugs, natural products, physiological compounds and environmental chemicals like pesticides, pollutants and pro-carcinogens) in human biology. Out of many existing isoforms of cytochrome P450, most of the reactions are undertaken by CYP2C9, CYP2C19, CYP2D6 and CYP3A4. The CYP3A4 is one of the most important of other cytochrome isoforms as approximately 60% of oxidized drugs are bio-transformed in its full or partial involvement (Yang, 2003), hence, to avoid the interference in its function by ligands being screened as oxazolidinones potentiators, this filter mechanism has been designed. Therefore, prior to docking the ligand library with the target Cfr, docking of ligand library was performed with CYP3A4 **(PDBID: 3UA1)** and further the screened ligands having lower binding energy with reference to one of its inhibitor ritonavir were sorted for further screening procedures.

3.4.3.3 Dock 1: Setting reference values for docking

Table 10: Molecular Docking reference values for filter proteins

Protein	Active sites	Grid box	Native ligand	Binding energy
hMAT1A (6SW5)	ALA55, GLU70, GLN112, GLN113, SER114, ILE117, GLY133, LYS289, ASP291	Center: X=31.096, Y=-0.571, Z=24.983 Dimensions: X=27.625, Y=57.151, Z=32.622	SAM and SAH	-7.9 and -7.2 Kcal/mol
Cytochrome P450 3A4	TYR53, PHE57, ASP76, ARG105, ARG106, PHE108, MET114, SER119, ILE120, LEU210, LEU211, PHE213, PHE215, THR224, PHE241, ILE300, ILE301, PHE304, ALA305, THR309, ILE369, ALA370, MET371, ARG372, LEU373, GLU374, CYS442, GLY481, LEU482	Center: X=23.819, Y=-30.803, Z=-19.366 Dimensions: X=28.368, Y=28.403, Z=26.540	Ritonavir SAM and SAH	-10.4 Kcal/mol -7.4 and -7.3 Kcal/mol

3.4.3.4 Dock 2: Final docking against target protein Cfr

Two rounds of docking were performed, initially, exhaustive and number of modes were set as 8/16, followed by the screened ligands again docking with 32/32 exhaustiveness and number of modes parameter for more specific conformation.

Table 11: Molecular Docking reference values for target proteins

Protein	Active sites	Grid box	Native ligand	Binding energy
Cfr; Gasteiger charge added: 0.0016	PHE118, CYS119, MET155, GLY156, MET157, GLY158, GLU159, SER189, THR190, SER212, HIS214, ILE290, ASN293, ARG327	Center: X = -9.436 Y = 1.384 Z = 2.646 Dimensions: X = 18.408 Y = 24.14 Z = 23.165	SAM and SAH	-8.2 and -8.4 Kcal/mol Cut off = -8.2

3.4.4 Docking result analysis

The final results obtained by docking a filtered ligand library with the target resistance element Cfr were then sorted based on their higher binding energy and further studied for protein ligand interaction.

3.4.4.1 Interactions of ligands and protein target

The interaction between lead compound and protein target were analyzed using Discovery Studio Visualizer. The bonds associated in the interaction, feasibility, and other factors such as bond length and interacting forces were studied. In addition, the hydrophobic bonding and its interaction was also assessed for stable association of lead to the binding pocket of the target molecule.

3.4.4.2 Bond type visualization and analysis

The analysis of the bond type in the interaction between respective ligands with the target was done using BIOVIA Discovery Studio Visualizer.

3.4.4.3 Hydrophobic bond interactions

The hydrophobic bond interaction between protein and lead compounds were investigated using Ligplot+ software.

4. RESULT AND DISCUSSION

4.1 Secondary metabolite activity testing

4.1.1 Primary culture, colony study and isolation

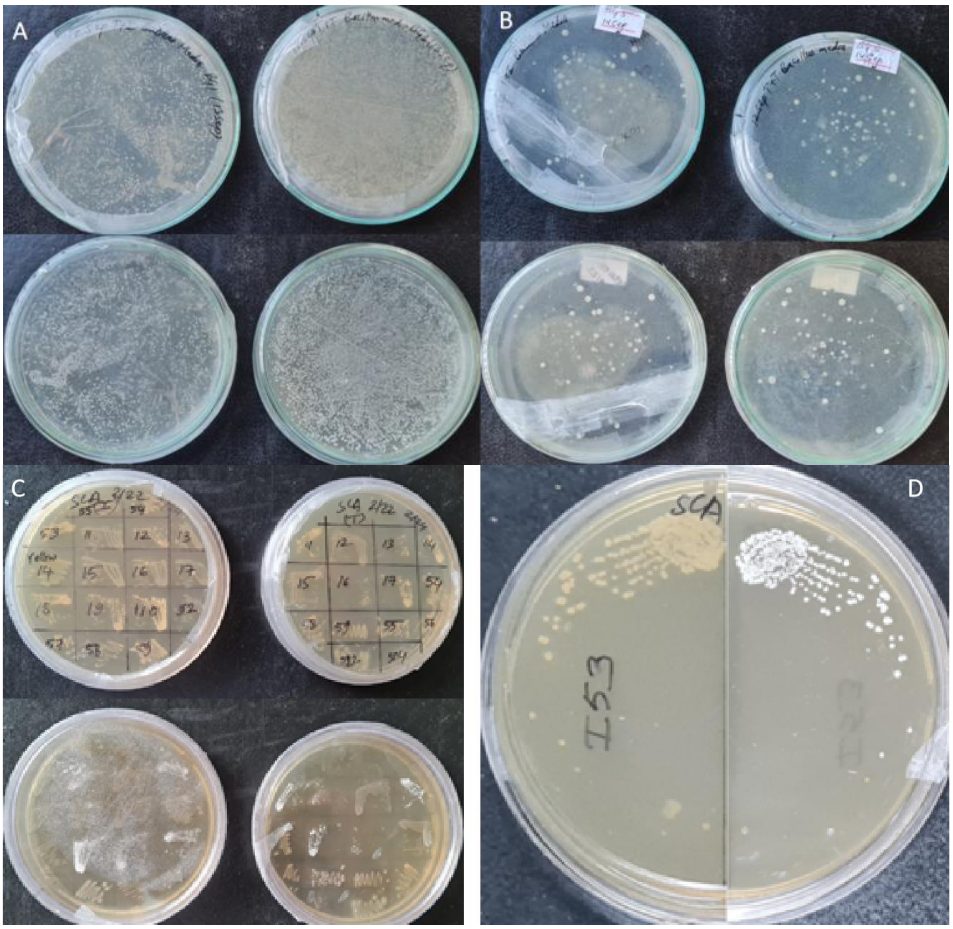

Figure 3: Spread plate in Bacillus modified media BG1 (A), BG5 (B), Screening in Starch Casein Agar plate (C) and I53 in ISP2 (D)

The less severe heat treatment method for a relatively short time was adopted to limit the growth of fast-growing spore-forming organisms from the soil sample. Out of the 9 different samples processed, only two samples showed traces of powdered, dry Streptomyces like colonies. Other samples however did not show the *Streptomyces* like growth but rather different *Bacillus* kind of growth. Hence, to confirm all the different Streptomyces like and bacillus like colonies, 31 different isolates were sub cultured in SCA agar plate. From here, the nine powdery, chalky and dry colonies were selected to proceed further test and antimicrobial extraction for activity assessment.

4.1.2 Macroscopic colony identification and gram staining

All the 9 isolates' colonies were powdery and chalky. The isolate I53 however had a distinct fresh musty odor of soil. Other isolates however had a faint odor of dry soil. Gram staining results showed that all the isolates were gram positive and retained the purple color of Crystal violet with highly branched filamentous structure.

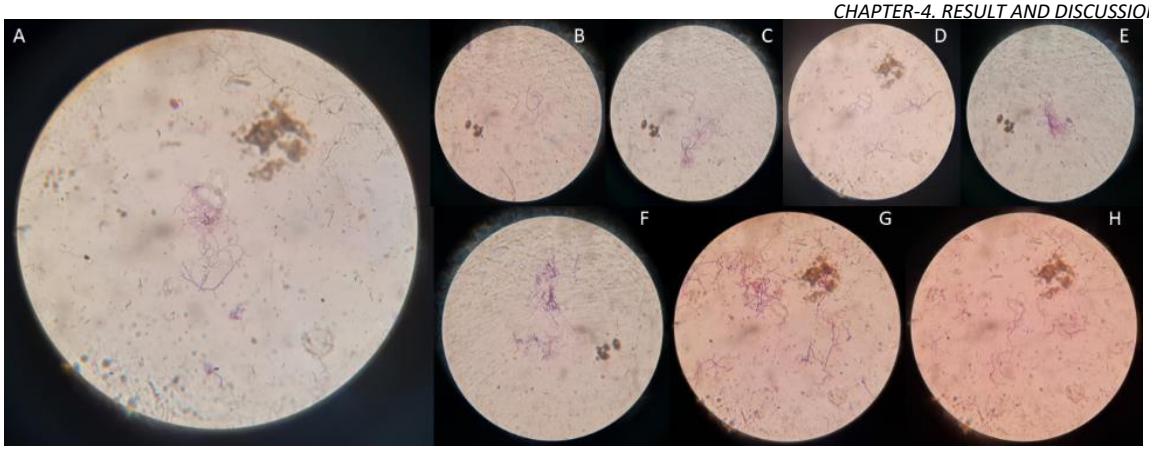

Figure 4: Gram Staining under 100X magnification (A- I53), (B- T17), (C- I19), (D- T14), (E- I110), (F- T12), (G-T13) and (H-T11)

4.1.3 Enzymatic Assay

The results of enzymatic assay are summarized in figures and table below.

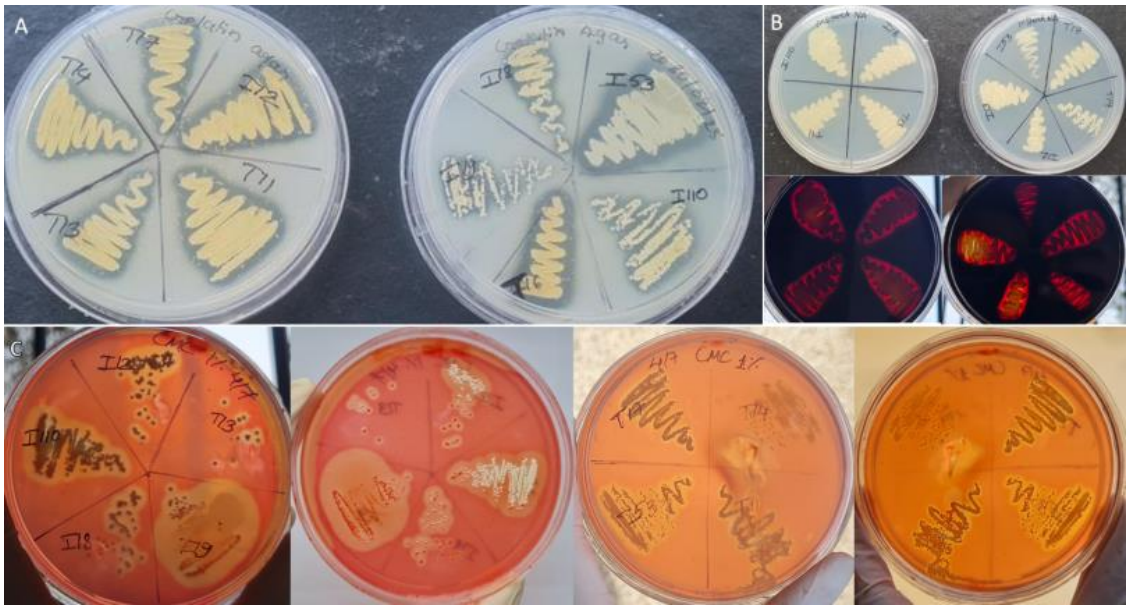

Figure 5: Enzymatic Assay- Gelatin hydrolysis test (A), Starch hydrolysis test (B), Cellulose hydrolysis test (C)

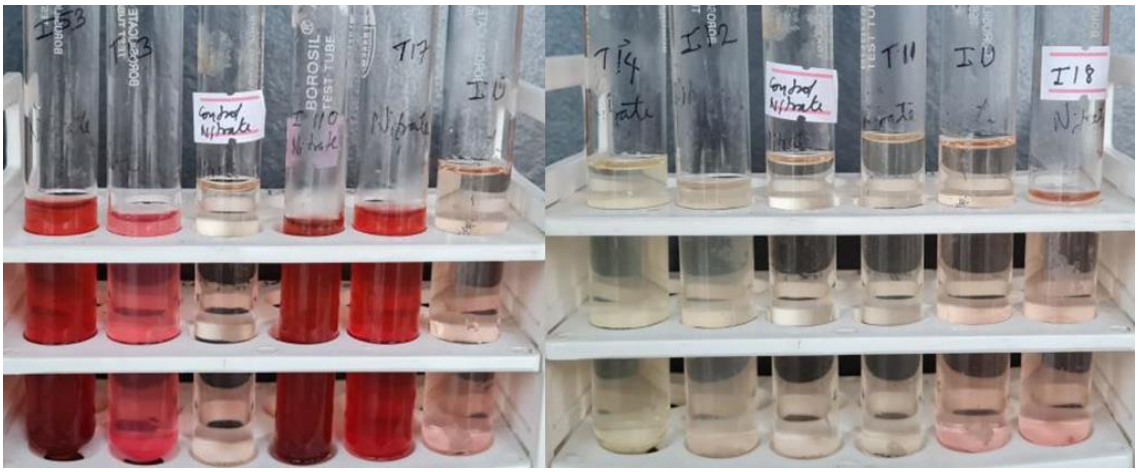

Figure 6: Nitrate Reduction Test

The summary of enzymatic assay is in the table below.

Table 12: Biochemical enzymatic assay

Isolate/Substrate	Starch	Cellulose	Gelatin	Nitrate
T11	+	+	+	-
I12	+	+	+	-
T13	+	+	+	+
T14	+	-	+	-
T17	+	+	+	+
I18	+	+	+	-
I19	+	+	-	-
I110	+	+	+	+
I53	+	+	+	+

For starch hydrolysis, all the isolates were positive. Similarly, for cellulose and gelatin hydrolysis tests, all isolates showed positive results except T14 and I19 respectively.

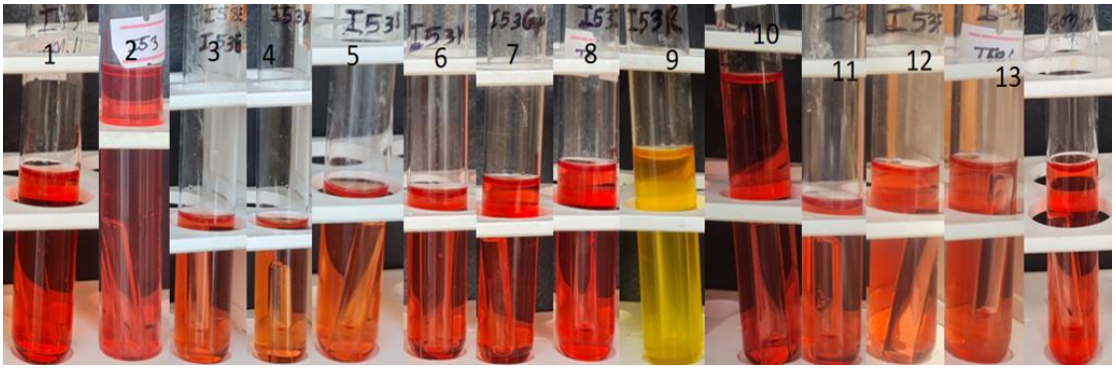

Figure 7: Carbohydrate Utilization test of isolate I53; from left: Melibiose (1), Sucrose (2), Erythritol (3), Xylose (4), Sorbitol (5), Maltose (6), Galactose (7), Inositol (8), Ribose (9), Mannitol (10), Lactose (11), Fructose (12), Glucose (13) and control (14)

Furthermore, the full carbohydrate utilization results are documented in the table below.

Table 13: Carbohydrate Utilization test

Isolate/Carbohydrate	1	2	3	4	5	6	7	8	9	10	11	12	13
T11	-	+	+	+	-	+	-	-	-	-	-	-	-
I12	+	+	+	+	+	+	+	+	+	+	+	+	+
T13	+	+	+	+	+	+	+	+	+	+	+	+	+
T14	+	+	+	+	+	+	+	+	+	+	+	+	+
T17	+	+	+	+	+	+	+	+	+	+	+	+	+
I18	+	-	+	+	+	+	+	+	+	+	+	+	+
I19	+	-	+	+	+	+	+	+	+	+	+	+	+
I110	-	-	-	+	-	-	-	-	-	-	-	-	-
I53	-	-	-	-	-	-	-	-	+	-	-	-	-

From the overall biochemical assay, we can imply that all the 10 isolates are different as none of them display the same set of assay results.

4.1.4 Primary screening

In primary screening, all the isolates showed antimicrobial activity against ATCC *E. coli* and ATCC *Staphylococcus aureus* with Partial or complete line of inhibitions. This may be due to the modification of media with tannic acid and indole, robust antibiotic producing bacteria were able to grow, limiting unwanted growth since tannic acid is a polyphenol stress inducing compound with antibacterial properties beyond a prescribed concentration.

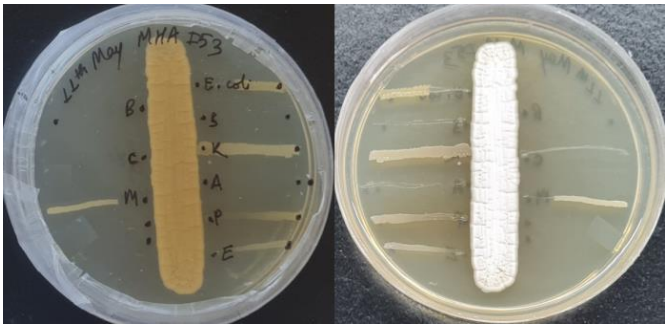

Figure 8: Perpendicular Streak Plate technique for primary screening

The isolate I53 showed inhibition of ATCC *E. coli* and ATCC *Staphylococcus aureus*. Similarly, K, A, P, E, C, and M represent hospital samples of *Klebsiella, Acinetobacter, Proteus, Enterococcus, Candida,* and MRSA 6721 respectively. B is not applicable.

4.1.5 Secondary metabolites and AgNP production

4.1.5.1 Antibiotic extraction

Figure 9: Secondary metabolite production

Figure 10: Antibiotic crude extract

Figure 11: Biogenic AgNP synthesis

4.1.5.2 Antimicrobial susceptibility plate assay

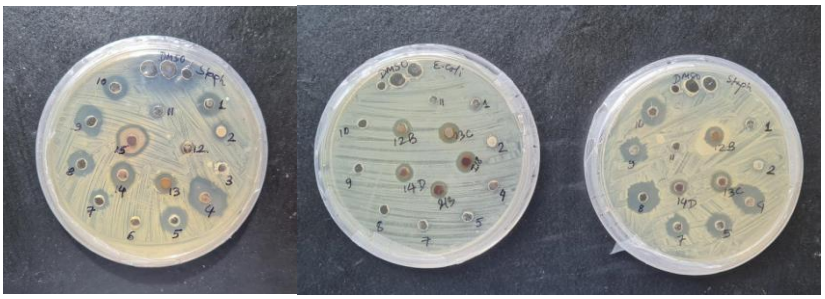

Figure 12: Antimicrobial susceptibility plate assay

In the first picture, the antibiotic stock solution was prepared in 100% DMSO. Similarly, in picture number 3, the stock solution was prepared using 50% DMSO. The stocks from 4 to 11 were extracted metabolites from isolate I53, Unknown, T14, I12, T17, I18, I110 and T13 in respective order. The 12, 13 and 14 were the AgNP samples synthesized from extracts of isolates T110, I12 and I53 respectively.

4.1.5.3 Resazurin antimicrobial assay of secondary metabolite

Table 14: ATCC strains AST standardization

Bacteria	Antibiotic	MIC reported in this study (µg/ml)	MIC recommended by CLSI (µg/ml)		
			S	I	R
Klebsiella pneumoniae 700603	Tetracycline	K9T= 7.8	≤4	8	≥16
Klebsiella pneumoniae 700603	Chloramphenicol	K10C= 3.9	≤8	16	≥32
Escherichia coli 25922	Tetracycline	E10T=3.9	≤4	8	≥16
Escherichia coli 25922	Chloramphenicol	E10C=3.9	≤8	16	≥32
Staphylococcus aureus 29213	Tetracycline	ST15=0.122	≤4	8	≥16
Staphylococcus aureus 29213	Chloramphenicol	SC15=0.122	≤8	16	≥32

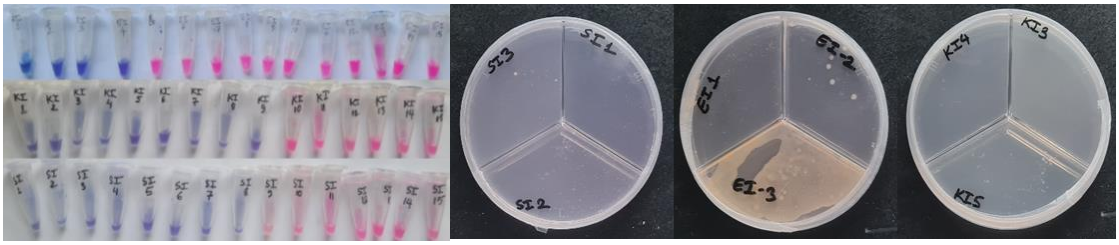

Figure 13: Determination of the (A) MIC and (B) MBC by resazurin based microdilution method of I53 extract against three standard strains

The MBC value of chloramphenicol for *E. coli*, *Klebsiella*, and *Staphylococcus* was E6C (1.97 mg/ml), K2C (31.67 mg/ml), SC3 (15.83 mg/ml) respectively and that of tetracycline was

E6T (1.97 mg/ml), K8T (0.494 mg/ml), and S5T (3.958 mg/ml) respectively. The MIC value of the I53 metabolite was determined by the resazurin broth dilution method. The MIC value of I53 antibiotic for *E. coli*, *Klebsiella*, and *Staphylococcus* was EI4 (7.91 mg/ml), KI9 (0.247 mg/ml), SI8 (0.49 mg/ml) with retention of blue-purple color of Resazurin. The purple color of resazurin is changed to pink as a result of intracellular reduction of resazurin to resorufin by viable and metabolically active cells (Präbst *et al*., 2017). However, the appropriate amount of resazurin dye should be used in this assay as it tends to give false positive results if used excessively. The MBC value for *Klebsiella*, and *Staphylococcus* was KI3 (15.83 mg/ml) and SI1 (63.33 mg/ml) respectively. However, The MBC value for *E. coli* was found higher than EI1 (63.33 mg/ml). Overall, the MIC values of the extract was much higher than the standard antibiotics chloramphenicol and tetracycline indicating lower efficacy and hence substandard. This might be due to the presence of various organic compounds in the extract apart from the antibiotic molecule, so the antibiotic produced might not have been in sufficient concentration. Hence antibiotic purification is necessary for accurate reliable results.

4.1.6 Molecular characterization of isolate

4.1.6.1 16S rRNA amplification

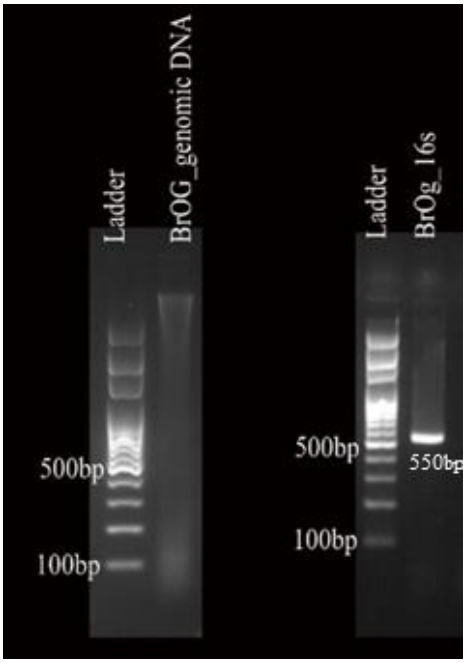

Figure 14: Molecular characterization of isolate- (A) genomic DNA band of I53 isolate, (B) 16S rRNA PCR product band

The band of genomic DNA of the isolate was visualized by agarose gel electrophoresis (on the left) and the 16S rRNA PCR product size was determined (on the right) with a band at around 550 bp.

4.1.6.2 Sequence alignment and phylogenetic tree construction

Sequencing BLAST Result:

S.No.		Query information	Blast Hit Information				
	Sample ID	Lab ID	Query Length	Query Cover %*	Identity%*	Scientific Name	Species Hits with Accessions No.
1	BrOG	TU01	175	100	100	*Streptomyces* sp.	OQ976971 (*Streptomyces rubiginosohelvolus*), OQ976906 (*Streptomyces griseus*), CP124863.1 (*Streptomyces* sp.)

Phylogenetic analysis

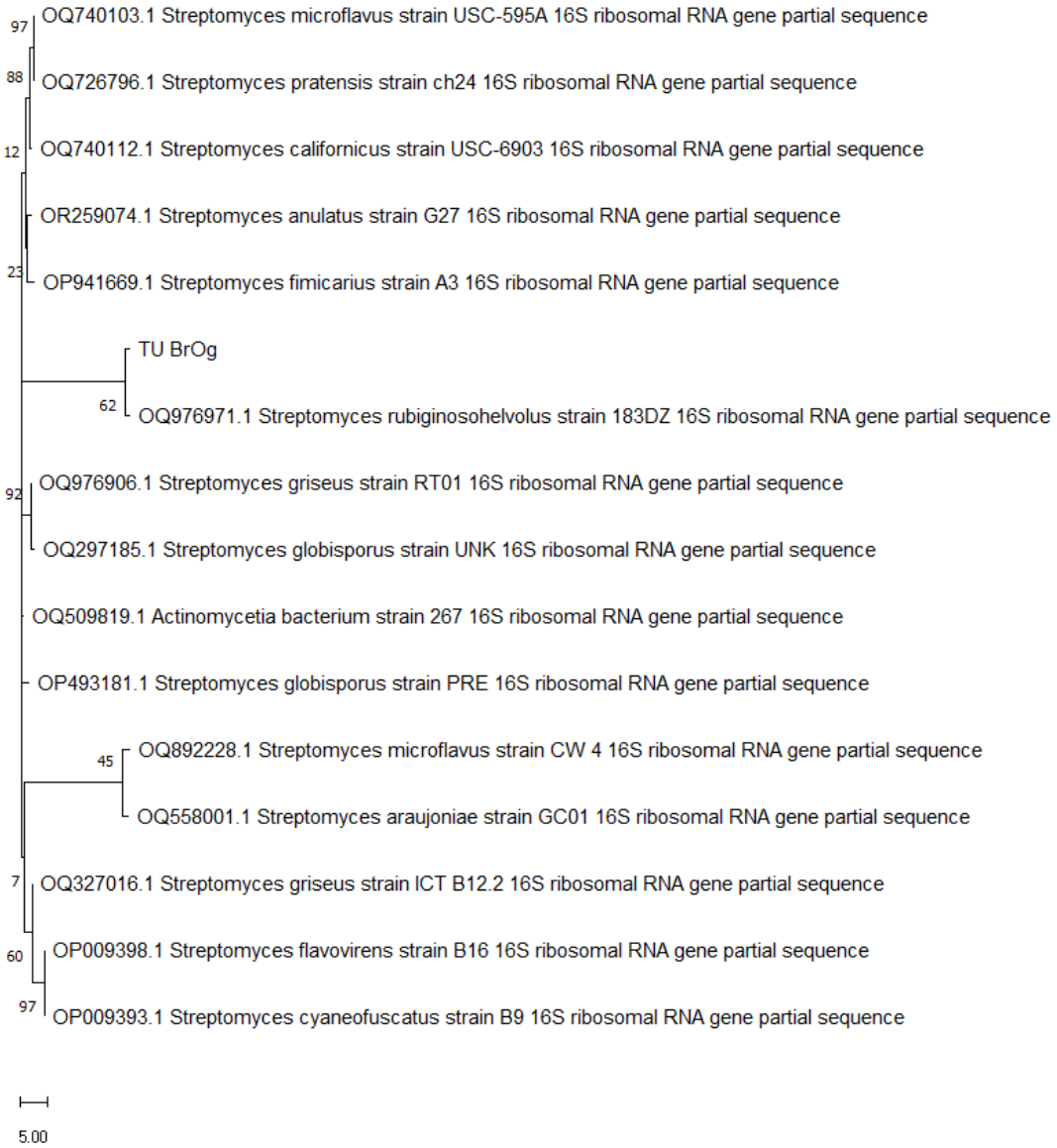

Figure 15: Phylogenetic tree of *Streptomyces* isolate I53

The sequence alignment using BLAST revealed 100% sequence identity of the I53 isolate with the *Streptomyces griseus* and *Streptomyces rubiginosohelvolus.* The Phylogenetic

analysis reveals the evolutionary relationship of unknown isolates with other organisms based on the genetic identity it shares with closely related descendants. Among several methods such as distance-matrix method (neighbour joining (NJ) or unweighted pair group method with arithmetic mean (UPGMA), maximum parsimony methods and maximum likelihood method, the maximum parsimony and maximum likelihood methods are reported to be the most accurate, though they take more time to run. Hence the method of maximum likelihood was employed to construct the phylogenetic tree (Price *et al*., 2010).

From the phylogenetic tree, the isolate I53 was found closely related to *Streptomyces rubiginosohelvolus* strain 183DZ as represented by the tree above. The isolate exhibited clade formation with *Streptomyces rubiginosohelvolus* strain 183DZ and showed a genetic divergence of 62 with its sister descendant.

4.2 Biogenic AgNP activity testing

4.2.1 UV-vis spectrophotometer analysis

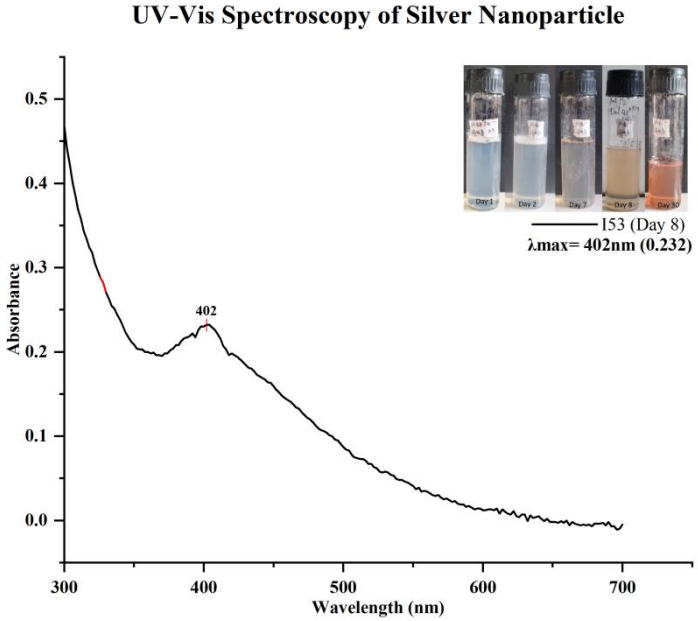

Figure 16: UV–Visible spectrum of silver nanoparticles from I53 isolate extract.

The Extract-$AgNO_3$ solution started changing its color to brownish from the third day of incubation and after a month the solution changed to a complete brown color. The presence of extracellular silver nanoparticle synthesis was confirmed with this color change, from colorless or slight yellow to brown. The brown color of the AgNP might be a result of $AgNO_3$ being reduced and the excitation of surface plasmon resonance (SPR) action being activated (Mulvaney, 1996). Furthermore, presence of silver nanoparticle was confirmed by UV–Vis spectrometry, with distinctive peak (absorbance maximum) detection at 402 nm, because silver nanoparticles absorb electromagnetic waves in 400 – 470 nm (Souri *et al*., 2023; Wypij *et al*., 2018). Moreover, the peak is satisfactorily sharp indicating good degree of nanoparticle dispersion as the broader peaks of nanoparticles

suggest nanoparticle aggregation which determine antibacterial efficacy (Lee *et al*., 2010).

4.2.2 AgNP FTIR characterization

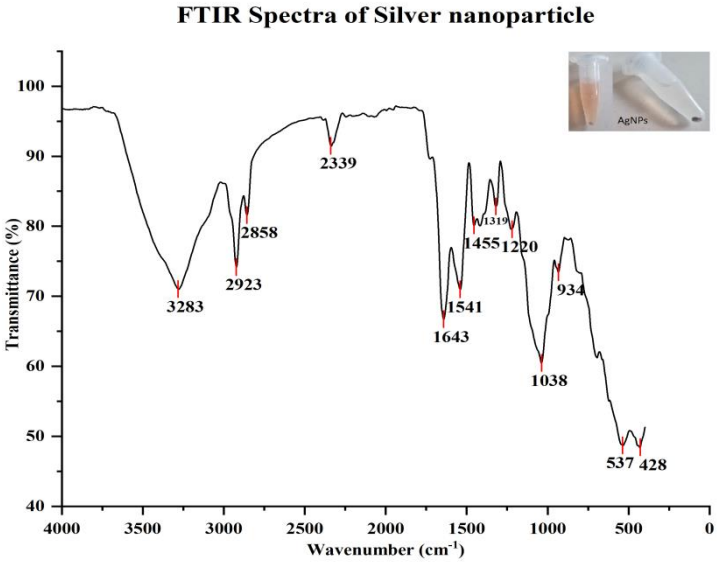

Figure 17: Fourier transform infrared spectroscopy analysis of AgNPs from I53 isolate extract. Absorbance bands: 3283, 2923, 1643, 1541, 1319, and 1038 cm^{-1}

The FTIR analysis of biogenic AgNPs synthesized from I53 isolate showed distinctive absorbance bands at 3283 cm^{-1} indicating O–H stretching in carboxylic acid groups, 2923 cm^{-1} C–H stretching in alkane groups, 1643 cm^{-1} C=N stretching in imine/oxime groups, 1541 cm^{-1} N–O stretching in nitro compound groups, 1319 cm^{-1}O–H bending in phenol groups and 1038 cm^{-1} C–O stretching in vinyl ether groups (Libretexts, 2020). These findings suggest the extract contains imine or oxime, phenol and vinylic ether groups which might be responsible for its antimicrobial activity and its role as reducing agent for AgNP synthesis. This result concludes that AgNP was capped with the organic compounds with the bonds mentioned above and the phenol group might be responsible for reducing $AgNO_3$ to metallic silver nanoparticle (Jacob *et al*., 2007).

4.2.3 AgNP resazurin antimicrobial assay for MIC MBC determination

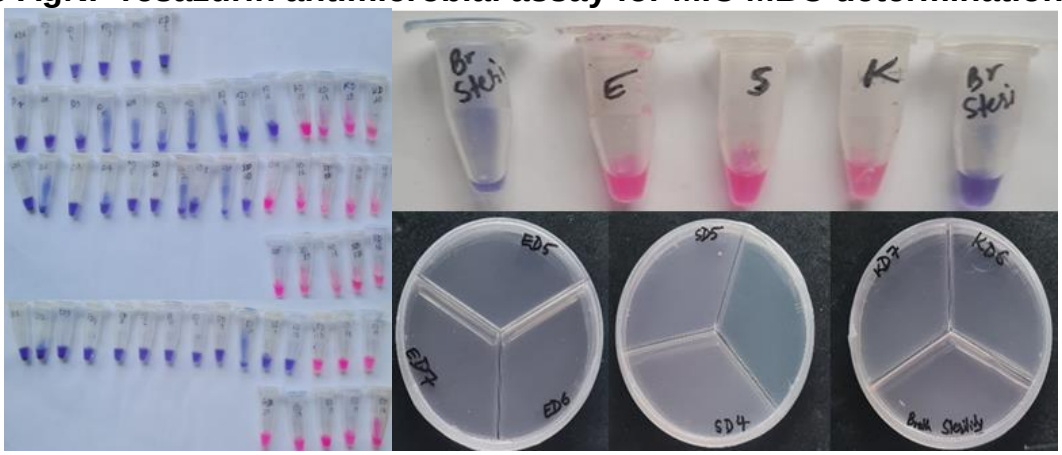

Figure 18: Determination of the (A) MIC and (B) MBC by resazurin based microdilution method of AgNP from I53 extract against three standard strains

The MIC value of AgNP determined by Resazurin broth dilution method for *E. coli*, *Klebsiella*, and *Staphylococcus* was ED12 (16 µg/ml), KD16 (0.1 µg/ml), SD10 (6.5 µg/ml) with retention of blue-purple color of Resazurin. Similarly, the MBC value for *Klebsiella*, *Staphylococcus* and *E. coli* was found KD7 (52 µg/ml), SD4 (0.416 mg/ml) and ED5 (0.104 mg/ml) respectively. The bacterial sensitivity towards synthesized AgNP was found higher than the isolate's crude extract. However, the AgNP antimicrobial susceptible was found significantly lower than the susceptibility shown by AgNP in other similar researches (De Los Ángeles Quinteros *et al*., 2016). This might be due to the size dependent antimicrobial efficacy factor of AgNP (Agnihotri *et al*., 2014), the AgNP formed was not sufficiently smaller to effectively inhibit or kill the test organisms in lower concentration. Overall, the MIC values of the biogenic AgNP was slightly higher than the standard antibiotics chloramphenicol and tetracycline indicating satisfactory efficacy and hence standard.

4.3 In silico potentiator screening against Cfr

4.3.1 Target selection and preparation

4.3.1.1 3D crystal structure search and building

The alignment result of Cfr with RlmN using the BLAST tool in NCBI showed 33.61% sequence similarity which is greater than the 30% identity usually required at the least to carry out homology modeling. Since the Alphafold also uses a deep-learning homology modeling based on a trained neural network, this factor needs to be considered. In addition, the low sequence similarity between the two proteins might be due to the less relatedness of the organism (Cfr from *Staphylococcus aureus* and RlmN from *E. coli*) from which the two proteins were extracted.

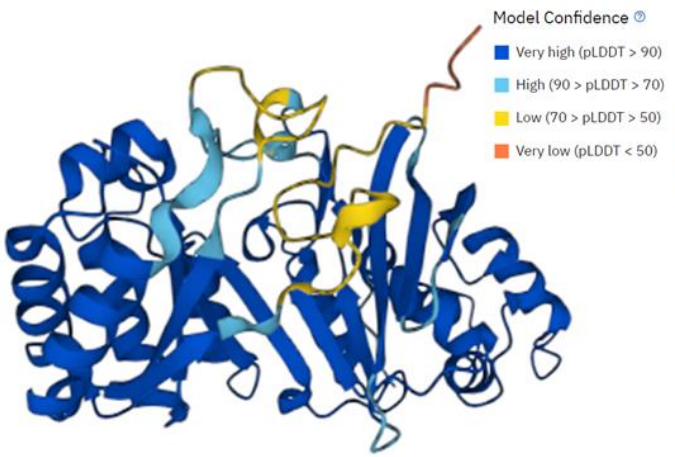

Figure 19: 3D structure of Cfr (Alphafold2)

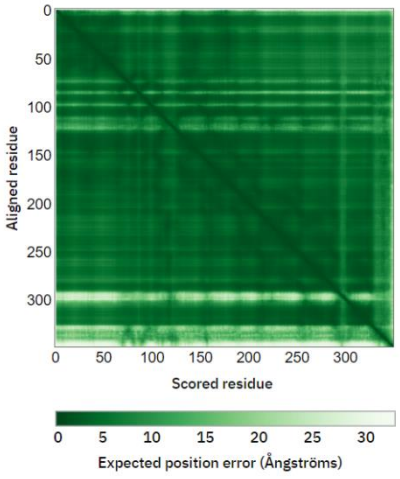

Figure 20: Predicted aligned Error (PAE)

The PAE plot is an error prediction in the constructed model. The shade of green indicates the expected distance error in Ångströms (Å), ranging from 0 Å to an arbitrary cut-off of 31 Å. The color at (x, y) corresponds to the expected distance error in the residue x's position when the predicted and the true structures are aligned on residue y. A dark green tile corresponds to a good prediction hence low error, whereas a light

green tile indicates poor prediction and high error.

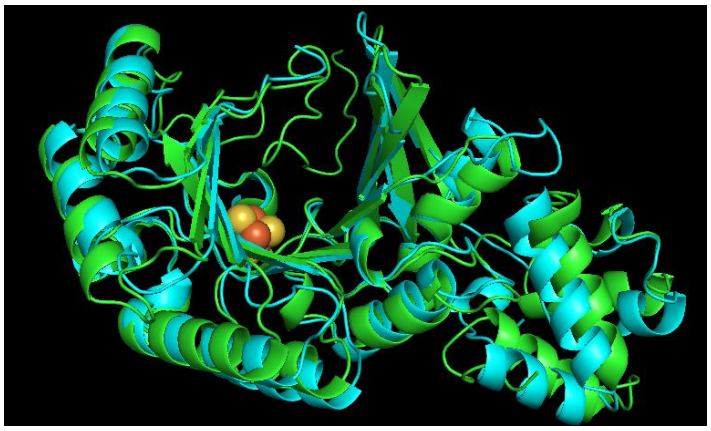

Figure 21: 3D structure of Cfr (Cyan) and its homolog RlmN (Green) alignment and visualization in Pymol

The primary and secondary protein motifs were similar when aligned together in Pymol. The active site residues predicted by Alphafold-Uniprot were perfectly matching as indicated in the following figure**.**

```
AMN16502.1      -----------------MNFNNKTKYGKIQEFLRSNNEPDYRIKQITNAIFKQRISRFED 43
3RFA            MSEQLVTPENVTTKDGKINLL-DLNRQQMREFFKDLGEKPFRADQVMKWMYHYCCDNFDE 59
                             :*:  . :  :::**::. .*  :* .*: : :::   ..*::

AMN16502.1      MKVLPKLLREDLINNFGETVLNIKLLAEQNSEQVTKVLFEV-SKNERVETVNMKYKAGWE 102
3RFA            MTDINKVLRGKLKEVAEIR--APEVVEEQRSSDGT-IKWAIAVGDQRVETVYI-PEDDRA 115
                *. : *:** .* :          ::: **.*.: * : : :   ::***** :  : .

AMN16502.1      SFCISSQCGCNFGCKFCATGDIGLKKNLTVDEITDQVLYFHLL--------GHQIDSISF 154
3RFA            TLCVSSQVGCALECKFCSTAQQGFNRNLRVSEIIGQVWRAAKIVGAAKVTGQRPITNVVM 175
                ::*:*** ** : ****:*.: *:::** *.** .**     :         : * .: :

AMN16502.1      MGMGEALANR-QVFDALDSFTDPNLFALSPRRLSISTIGIIPSIKKITQEYPQVNLTFSL 213
3RFA            MGMGEPLLNLNNVVPAMEIMLDDFGFGLSKRRVTLSTSGVVPALDKLGD-MIDVALAISL 234
                ***** * *  :*. *:: : *   *.** **:::** *::*::.*: :   :* *::**

AMN16502.1      HSPYSEERSKLMPINDRYPIDEVMNILDEHI---RLTSRKVYIAYIMLPGVNDSLEHANE 270
3RFA            HAPNDEIRDEIVPINKKYNIETFLAAVRRYLEKSNANQGRVTIEYVMLDHVNDGTEHAHQ 294
                *:* .* *.:::***.:* *: .:  : .::   . .. :* * *:**  ***. ***::

AMN16502.1      VVSLLKSRYKSGKLYHVNLIRYNPTISAPEMYGEANEGQVEAFYKVLKSAGIHVTIRSQF 330
3RFA            LAELLKDT-----PCKINLIPWNPFPGAP--YGRSSNSRIDRFSKVLMSYGFTTIVRKTR 347
                :..***.        ::*** :**  .**  **.:.:.::: * *** * *: . :*.

AMN16502.1      GIDIDAACGQLYGNYQNSQ-------------------------------------    349
3RFA            GDDIDAACGQLAGDVIDRTKRTLRKRMQGEAIDIKAVGNSSSVDKLAAALEHHHHHH   404
                * ********* *:  :
```

Figure 22: Cfr and RlmN (3RFA) sequence alignment (using Clustal omega)

From the results obtained from Clustal omega multiple sequence alignment, the active site residues were PHE118, CYS119, MET155, GLY156, MET157, GLY158, GLU159, SER189, THR190, SER212, HIS214, ILE290, ASN293, ARG327.

4.3.1.2 Target 3D structure validation

Before conducting computational experiments in the theoretical or experimental

protein models freely available in the internet and databases, first it needs to be assessed for its accuracy and reliability. Overall, the z-score is considered a standard quality assessment parameter that indicates the model quality and measures the deviation of total energy of the structure with reference to an energy distribution derived from random conformations. The Z-value outside a range characteristic for native protein imply an inaccurate structure.

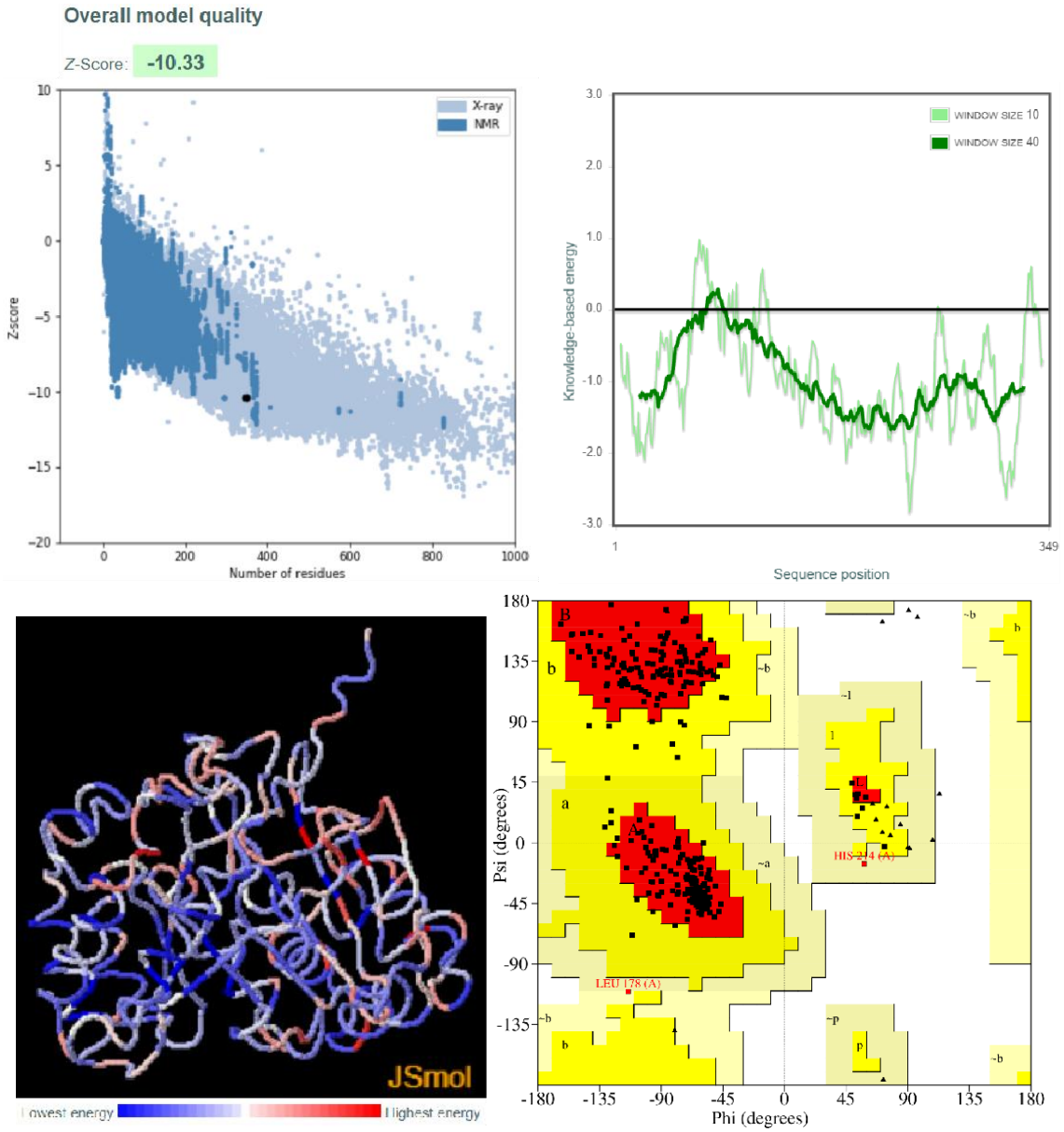

Figure 23: 3D structure validation- The Z-plot (A), energy plot (B), energy indicative/representative Cfr protein structure (C) and Ramachandran plot (D)

The z-score for 3RFA and Cfr (A) was -10.65 and -10.33 respectively. Both the structures were found within the range of structures obtained from X-ray sources. However, the structures were found inconsistent with the structure range obtained from NMR. Similarly, the energy plot of 3RFA indicated a perfect fit model quality with no amino acid sequence position indicating any positive value. On the contrary, the energy plot (B) of Cfr signifies few erroneous parts in the structure used with few amino acid sequence

positions indicating positive value. Furthermore, stereochemistry is another factor that determines the accuracy of the protein model which is determined by examining bond geometry in a Ramachandran plot. Certain conformation of phi and psi angles are forbidden in protein structures due to steric hindrance. Hence, a model which possesses 90% of its residues in the allowed regions of Ramachandran plot is regarded as a workable accurate model (Sumitha *et al*., 2020). The 93% and 91.1% (D) of residue of 3RFA and Cfr respectively occurred in the allowed region, hence both the targets were fit models. Therefore, the Cfr was moved forward towards further experiments.

4.3.2 Ligand preparation

4.3.2.1. ADME/TOX filter

After applying ADME/TOX filter, a natural product library of 2,24,205 narrowed down/reduced to 35,534.

4.3.2.2. Filter 1 and Filter 2

Screening the resultant ligand library further by docking against HMAT1A protein (11,970) and human cytochrome p450 Cyp3A4 protein, 9978 ligands remained.

4.3.3 Molecular Docking against Cfr

Further docking 9978 ligands with Cfr, 1195 ligands passed the screening, hence based on its binding energy the following compounds ZINC30884104, ZINC72320745 and ZINC22654022 were sorted as top three hits for potential potentiator.

4.3.4 Docking result analysis

The top hits were selected based on its binding affinity with the target Cfr as shown in the table below.

Table 15: Binding affinity of prioritized hits against target Cfr

Ligands	Zinc ID	Pubchem cid	Binding affinity against Cfr
ZINC30884104	ZINC000030884104	38031761	-9
ZINC72320745	ZINC000072320745	71692944	-9
ZINC22654022	ZINC000022654022	46084452	-8.8
Native ligands SAM/SAH			-8.2

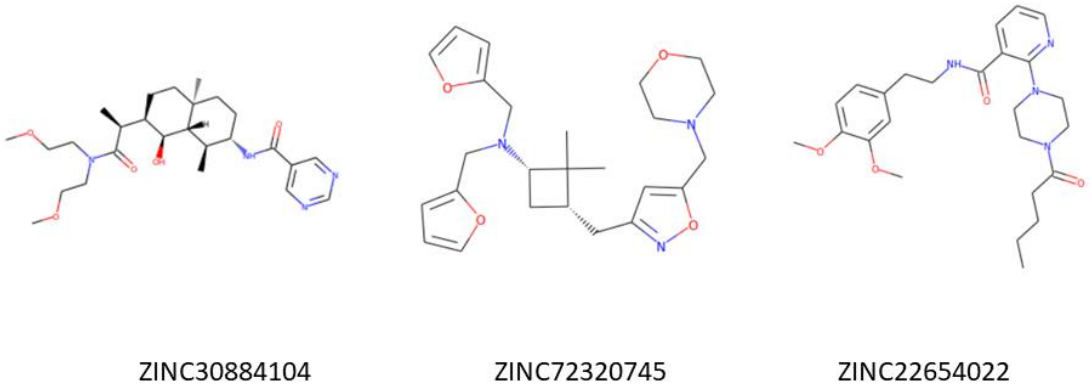

Figure 24: Structure of Lead compounds

4.3.4.1. Interactions of ligands and protein target

The top three screened leads were further selected to study their interaction with the protein by visualization and identification of protein amino acid residues involved in binding with ligand in the active binding site/cavity which was achieved by analyzing protein ligand interaction within 5 angstroms of the ligand and active binding site of the protein. The figure below shows the binding of target protein residues with respective ligands within distance of $5A^0$ and the table following summarizes the ligand interactions with various amino acid residues of the protein molecule.

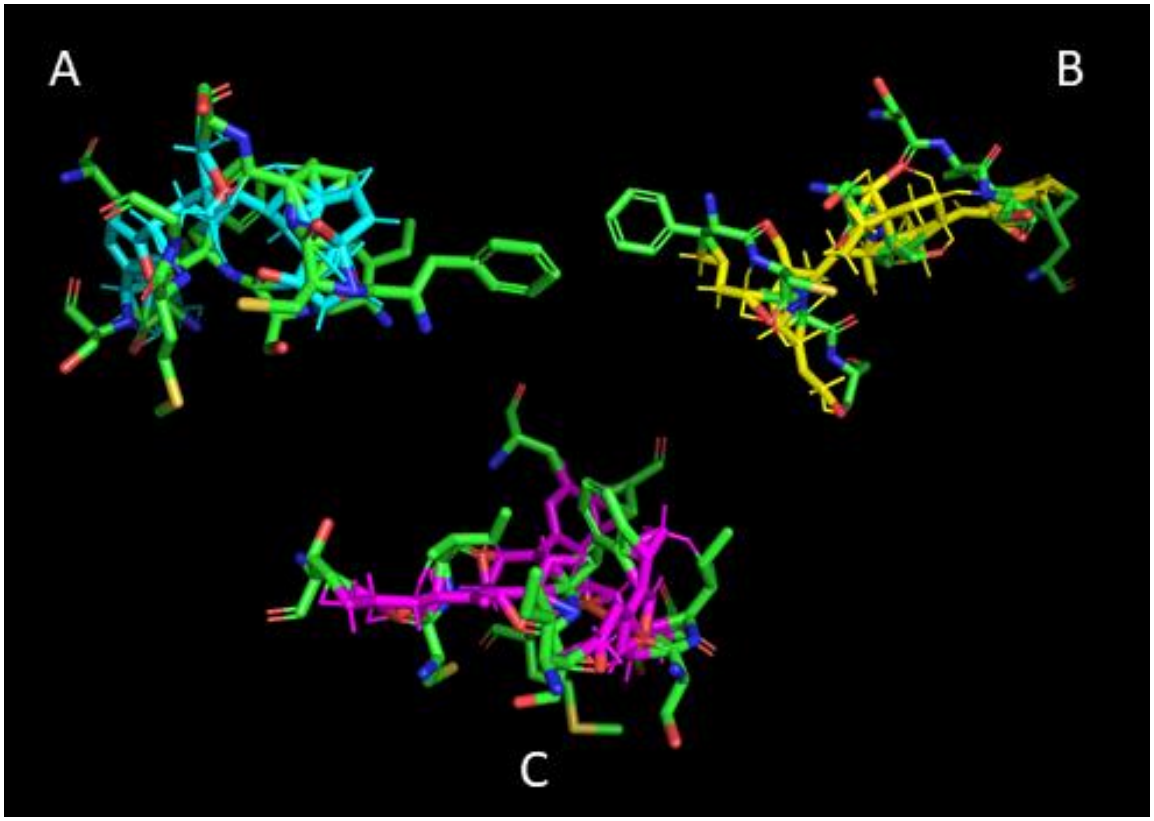

Figure 25: Cfr Protein interaction within $5A^0$ with ZINC72320745 [14897-cfr-sf4] (ligand in cyan) (A), ZINC30884104 [28644-cfr-sf4] (ligand in yellow) (B), and ZINC22654022 [30911-cfr-sf4] (ligand in magenta) (C) (using Pymol).

Table 16: Ligand-protein interaction of top hit ligands

Ligands	Amino acid residues of cfr (within 5 A^0)
ZINC72320745	E91, T92, V93, N94, M95, S103, F104, C105, I106, S107, S108, Q109, I135, Q138, V139, F142, S151, I152, S153, F154, M155, G156, M157, G158, E159, A160, L161, V166, L170, F173, L186, S187, I188 S189 T190, I200, V207, N208, L209, T210
ZINC30884104	V90, E91, T92, V93, N94, S103, F104, C105, I106, S107, S108, I135, Q138, V139, F142, I149, S151, I152, S153, F154, M155, G156, M157, E159, A160, L161, V166, F173, L186, S187, I188, S189, T190, S196, I197, I200, N208, L209, T210, L341
ZINC22654022	E91, T92, V93, N94, S103, F104, C105, I106, S107, S108, Q109, Q138, V139, F142, S151, I152, S153, F154, M155, G156, M157, G158, E159, A160, L161, A162, N163, V166, L170, R185, L186, S187, I188, S189, T190, V207, N208, T210

From the ligand interaction assessment with the target molecule, two residues namely Methionine and Serine at position 155 and 189 respectively were found actively interacting /mainly involved in the binding of ligand to the protein. These residues M155 and S189 might be the part of potential catalytic Met-His dyad and triad Ser-His-Glu here respectively. Though the Met-His dyad combination has not been reported previously, the methionine has been found playing a catalytic role via positively charged histidine stabilization (Ranaghan *et al*., 2014). Similarly, varied involvement of serine residue in combination with various other amino acids like histidine, Threonine, Cysteine, Aspartic acid, Glutamate and others in the catalytic triad has been reported (Ekici *et al*., 2008). The glutamate doesn't usually occur in classic serine peptidases though it is chemically equivalent to aspartate. However, in few hydrolytic enzymes such as lipase and acetylcholinesterase, the catalytic aspartate residue has been found replaced by glutamate (Polgár, 2005). Since most of the serine peptidase are able to cleave amide bond, serine peptidase triad Ser-His-Glu also might have conferred resistance to chloramphenicol and florfenicol like antibiotics by amide bond cleavage in respective antibiotics (Mahesh *et al*., 2018). As ineffectiveness of beta-lactam antibiotics has also been reported due to the hydrolysis of amide bond of beta lactam ring (Tooke *et al*., 2019), the chloramphenicol resistance mechanism might also involve hydrolysis of amide bond in chloramphenicol and florefenicol by Cfr with involvement of Ser-His-Glu catalytic triad.

Similarly, significant involvement of the residues C105, I106, S153, F154 and I188 was also found in all the lead compounds. The combined interaction of these residues with the hits might be responsible for better binding affinity of the leads with the target as compared to the native ligand SAM and SAH.

4.3.4.2. Bond type visualization and analysis

The lead-target interaction can further be studied by analysis of existing bond nature between the atoms and molecules of the respective ligand and protein which is illustrated and presented in the following figure and table respectively.

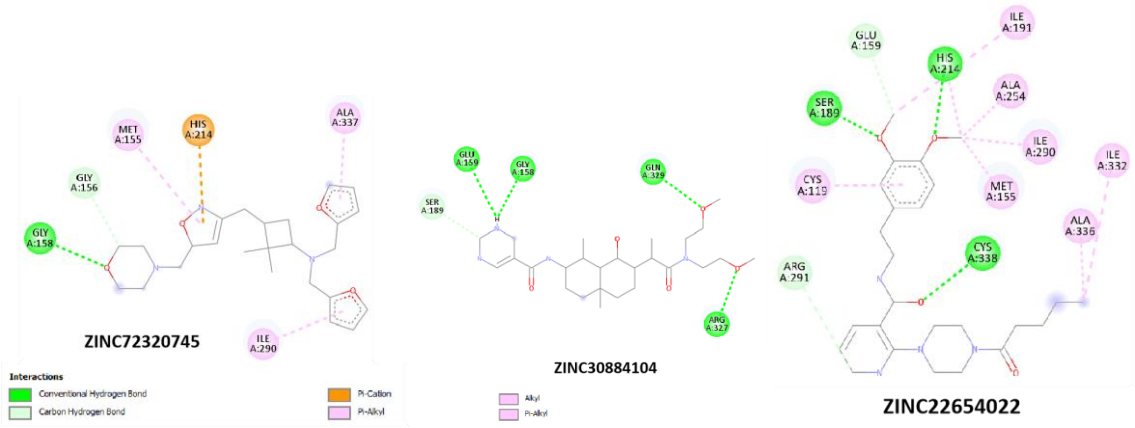

Figure 26: Bond types interaction with ZINC72320745 (A), ZINC30884104 (B), and ZINC22654022 (C) (using Discovery Studio).

In ligand ZINC72320745, molecular interaction was found facilitated by Pi-Alkyl bonding with three residues MET155, ILE290, ALA337; Carbon Hydrogen bonding with GLY156; Conventional H-bonding with GLY158 and Pi-cation interaction with HIS214. The compound ZINC30884104 showed interaction with target protein by majorly two types of bonding, namely Carbon Hydrogen bonding with SER189 and Conventional H-bond with four residues GLY158, GLU159, ARG327, and GLN329. Similarly, the third hit ZINC22654022 on the list exhibited molecular interaction through Conventional H-bonding with three residues SER189, HIS214 and CYS338; Carbon Hydrogen bonding with residues GLU159 and ARG291; Alkyl bonding with residues ILE191, ALA254, ILE332 and ALA336; and Pi-Alkyl bonding with residues MET155, CYS119 and ILE290. The Pi-cation bond might be the responsible factor here in ligand ZINC72320745 as Pi-cation interaction is regarded as a strong non-covalent interaction in aqueous solution important for ligand-protein interfaces and drug delivery (Bergsma *et al*., 2022). Furthermore, due to its role in molecular recognition, chemists has adopted the concept of pi-cation interaction in drug discovery process (Liang & Li, 2018).

Table 17: Ligand-protein interaction bond types of top hit ligands

Ligands	Amino acid residues	Interaction type
	MET155	Pi-Alkyl
	GLY156	Carbon Hydrogen bond
	GLY158	Conventional H-bond
	HIS214	Pi-cation
	ILE290	Pi-Alkyl
ZINC72320745	ALA337	Pi-Alkyl
	GLY158	Conventional H-bond
	GLU159	Conventional H-bond
	SER189	Carbon Hydrogen bond
	ARG327	Conventional H-bond
ZINC30884104	GLN329	Conventional H-bond
	MET155	Pi-Alkyl
	CYS119	Pi-Alkyl
	GLU159	Carbon Hydrogen bond
	SER189	Conventional H-bond
	ILE191	Alkyl
	HIS214	Conventional H-bond
	ALA254	Alkyl
	ILE290	Pi-Alkyl
	ARG291	Carbon Hydrogen bond
	ILE332	Alkyl
	ALA336	Alkyl
ZINC22654022	CYS338	Conventional H-bond

4.3.4.3. Hydrophobic bond interactions

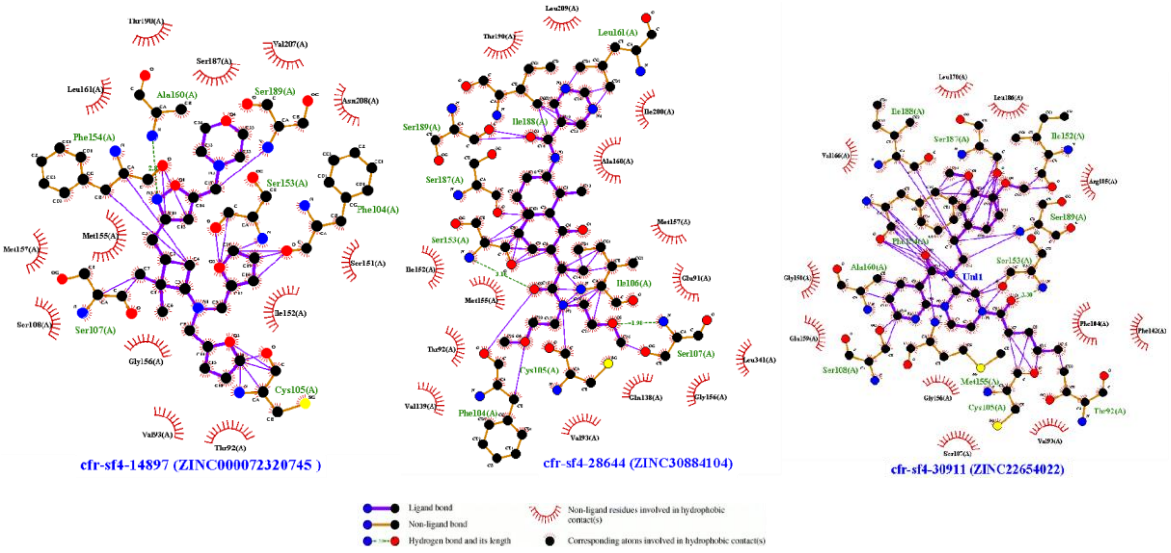

Figure 27: Hydrophobic interaction of residues with ZINC72320745, ZINC30884104, and ZINC22654022 (using Ligplot+)

Weak interactions like hydrogen bonding and hydrophobic interactions have been considered playing a crucial role in stabilizing lead compounds in the vicinity of protein structure (Patil *et al*., 2010). Additionally, they are involved in protein chaperoning

(Corbeski *et al*., 2022) and activation domain predictions (Kotha & Staller, 2023). Furthermore, hydrophobic interactions have been reported to enhance binding affinity in target-drug interfaces because binding affinity and drug efficacy are closely associated with hydrophobic interactions and have also been investigated for its optimization by including them at the site of hydrogen bonding (Qian *et al*., 2009). Therefore, increasing the number of hydrophobic atoms in the active core of drug-target interface increases the biological activity of the lead compound. On the contrary, the water molecule availability in hydrophobic regions also allows flexibility to this region.

From the protein-ligand interaction data obtained using ligplot+, ZINC72320745 exhibited hydrophobic interaction through thirteen hydrophobic residues Thr92, Val93, Ser108, Ser151, Ile152, Met155, Gly156, Met157, Leu161, Ser187, Thr190, Val207 and Asn208. Similarly, the residues involved in hydrophobic interactions with ZINC30884104 were Glu91, Thr92, Val93, Gln138, Val139, Ile152, Met155, Gly156, Met157, Ala160, Thr190, Ile200, Leu209, and Leu341. The ZINC22654022 showed hydrophobic interactions via eleven residues namely Val93, Phe104, Ser107, Phe142, Gly156, Gly158, Glu159, Val166, Leu170, Arg185, Leu186. The strong interaction of ZINC72320745 with the target might be due to its interaction with non-polar amino acids residues (namely alanine, valine, leucine, proline, methionine, tryptophan, glycine, isoleucine, and phenylalanine) of the target.

5. SUMMARY

Antimicrobial resistance is one of the greatest threats of today. In actuality, it is a natural phenomenon turned into a serious health crisis accelerated by human irresponsible actions. Cancer researchers around the world has claimed AMR undermining all the efforts and progress in their field of research. Every other health care problem has an AMR undertone. Hence, it is not a single problem but rather a problem woven in too many. To address this issue, an integrated AMR approach of computational potentiator screening against antimicrobial resistance element Cfr, and traditional production of antibiotic and AgNP from *Streptomyces sps.* was designed and pursued. The generalized screening protocol of ADMET and specified screening for essential hMAT1A and human cytochrome p450 cyp3A4, was employed by adjusting parameters and molecular docking respectively. In the process of specific screening, the molecular docking of respective proteins hMAT1A and cytochrome P450 3A4 was held with its reference native ligands SAM and SAH as well as first phase passed ligand library of Natural products. Further, the molecule having lower binding energy compared to native ligands were sorted and further docked against the target Cfr. A total of 1195 compounds yielded higher binding with Cfr than the native ligand SAM and SAH from this process. Based on the binding affinity, the top three hits namely ZINC72320745, ZINC30884104 and ZINC22654022 were identified. The ZINC72320745 structure revealed its furan scaffold.

With regards to traditional antimicrobial production, *Streptomyces* I53 was isolated and employed for antibiotic production simultaneously utilizing its cell free extract to synthesize AgNP. After AgNP characterization, antimicrobial susceptibility testing was conducted adopting resazurin microdilution method. The antibiotic extract showed lower inhibition against *Staphylococcus aureus* 29213 (MIC and MBC values of 0.49mg/ml and 63.33 mg/ml), *Klebsiella pneumoniae* 700603 (0.247 mg/ml and 15.83 mg/ml) and *E. coli* 25922 (7.91mg/ml and higher than 63.33 mg/ml) respectively as compared to the inhibition by AgNP with MIC of 6.5 µg/ml, 0.1 µg/ml and 16 µg/ml; and MBC of 0.416 mg/ml, 52 µg/ml and 0.104 mg/ml for respective test organisms.

Similarly, the Biogenic AgNP was characterized by UV-Vis spectroscopy with peak absorbance observed at 402 nm. Additionally, the FTIR analysis showed distinct absorbance bands suggesting presence of vinylic ether (1038 cm^{-1}), phenol (1319 cm^{-1}) and imine or oxime (1643 cm^{-1}) group in the extract, responsible for its antimicrobial and reducing property in AgNP synthesis.

6. CONCLUSION

The biochemical and molecular characterization of I53 isolate confirmed the bacteria was *Streptomyces.* Additionally, I53 isolate produced the antibiotic and was also successful in producing silver nanoparticle biogenically. The efficacy of biogenic AgNP was found higher as compared to extract alone which might be due to combinatorial effect of nanoparticle and the extract. Furthermore, the three hits ZINC72320745, ZINC30884104 and ZINC22654022 could be the potential Cfr inhibitor for its potential use as PhLOPS potentiators. Moreover, another resistance mechanism of Cfr might be the catalytic hydrolysis of antibiotics with the involvement of serine protease catalytic triad Ser 189, Glu159 and His214. Hence, due to the pi-cationic interaction with histidine and bond formation with serine and glutamate, the ligand ZINC72320745 might be more potent than the other two ligands.

Discovering a novel antibiotic from *Streptomyces* is a rigorous and resource intensive process. Having said that, despite the challenges, the quest for discovering new antibiotics should be continued and consistent effort is recommended. One of the approaches could be CADD mediated screening of new *Streptomyces sps*. for development of new and novel antibiotics. Appropriate soil sample site(s) selection could be taken for isolation of new *Streptomyces sps*. The media modification is a useful technique in screening potential isolate coalition with less severe treatment process such as moist heat treatment for a short period to minimize the growth of undesired bacteria. Similarly, components like casein, and lignin degradation products such as tannic acid, furfural can be used to modify media due to stress inducing properties of the compound and saprophytic nature of *Streptomyces*. Moreover, compounds like indole can be used to mimic the presence of fast-growing indole positive bacteria to accelerate antibiotic production. The biogenic AgNp has antimicrobial potential hence can be explored more. Similarly, the high throughput virtual screening can be adopted to narrow the lead molecule for practical and rational experimentation rather than the traditional approach of random hit and trial.

7. RECOMMENDATION

Therefore, it is recommended that these lead molecules be tested in vitro for AST against the target Cfr and further be pursued as potentiator molecules to develop combinatorial drugs. Similarly, respective enzymes inhibition kinetics could be studied. Furthermore, the molecules could be taken forward to animal testing and toxicity testing. Elaborate Cfr mutational analysis and its virtual screening or designing drugs for respective variants is recommended as evolved Cfr variants have been reported to confer enhanced antibiotic resistance (Tsai *et al*., 2022). Screening the bacteria for super resistant Cfr mutation can also be useful.

The modified media is also recommended to be further explored and optimized for isolation of *Streptomyces sps.* Additionally, stress inducing molecules can be explored more to trigger and maximize new antimicrobial production from *Streptomyces* and *Actinomycetes* isolates overall. Furthermore, antibiotic purification is also recommended for accurate reliable results.

The biogenic AgNp has antimicrobial potential however, the biogenic size controlling strategies can be developed by optimizing parameters to gain edge over physicochemical methods of silver nanoparticle synthesis.

Further metagenomics analysis of *Actinomycetes* from potential environment sources might open up avenues for antibiotic gene analysis and its mechanisms at the molecular level.

8. REFERENCES

Abraham, E. P., & Chain, E. (1988). An enzyme from bacteria able to destroy penicillin. 1940. *Reviews of infectious diseases*, *10*(4), 677-678.

Agnihotri, S., Mukherji, S., & Mukherji, S. (2014). Size-controlled silver nanoparticles synthesized over the range 5–100 nm using the same protocol and their antibacterial efficacy. *RSC Advances*, *4*(8), 3974–3983.

Alam, K., Mazumder, A., Sikdar, S., Zhao, Y., Hao, J., Song, C., Wang, Y., Sarkar, R., Islam, S., Zhang, Y., & Li, A. (2022). Streptomyces: The biofactory of secondary metabolites. *Frontiers in Microbiology*, *13*. https://doi.org/10.3389/fmicb.2022.968053

Arenz, S., & Wilson, D. N. (2016). Blast from the Past: Reassessing Forgotten Translation Inhibitors, Antibiotic Selectivity, and Resistance Mechanisms to Aid Drug Development. *Molecular Cell*, *61*(1), 3–14. https://doi.org/10.1016/j.molcel.2015.10.019

Arias, C. A., Vallejo, M. I., Reyes, J., Panesso, D., Moreno, J., Castañeda, E., Villegas, M. V., Murray, B. E., & Quinn, J. P. (2008). Clinical and Microbiological Aspects of Linezolid Resistance Mediated by the cfr Gene Encoding a 23S rRNA Methyltransferase. *Journal of Clinical Microbiology*, *46*(3), 892–896. https://doi.org/10.1128/jcm.01886-07

Baker, S. J., Payne, D. J., Rappuoli, R., & De Gregorio, E. (2018). Technologies to address antimicrobial resistance. *Proceedings of the National Academy of Sciences of the United States of America*, *115*(51), 12887–12895. https://doi.org/10.1073/pnas.1717160115

Bapat, R., Chaubal, T. V., Joshi, C., Bapat, P. R., Choudhury, H., Pandey, M., Gorain, B., & Kesharwani, P. (2018). An overview of application of silver nanoparticles for biomaterials in dentistry. *Materials Science and Engineering: C*, *91*, 881–898. https://doi.org/10.1016/j.msec.2018.05.069

Bergsma, S., Poulios, E., Charalampogiannis, N., Andraws, O., & Achinas, S. (2022). Cation-Π Interaction as a Key Player in Healthcare: A Mini-Review. *Digital Medicine and Healthcare Technology*, *2022*, 1–13. https://doi.org/10.5772/dmht.11

Carrara, E., Grossi, P., Gori, A., Lambertenghi, L., Antonelli, M., Lombardi, A., Bongiovanni, F., Magrini, N., Manfredi, C., Stefani, S., Tumbarello, M., Tacconelli, E., Auerbach, N., Cassol, C., Rancan, L., Mangioni, D., Ungaro, R., Postorino, S., & Vargas, J. (2024). How to tailor recommendations on the treatment of multi-drug resistant Gram-negative infections at country level integrating antibiotic stewardship principles within the GRADE-ADOLOPMENT framework. *The Lancet Infectious Diseases*, *24*(2), e113–e126. https://doi.org/10.1016/s1473-3099(23)00435-8

Chawla, M., Verma, J., Gupta, R., & Das, B. (2022). Antibiotic Potentiators against Multidrug-Resistant Bacteria: Discovery, development, and Clinical Relevance. *Frontiers in Microbiology*, *13*. https://doi.org/10.3389/fmicb.2022.887251

Chiang, Y., Chang, S., Oakley, B. R., & Wang, C. C. C. (2011). Recent advances in awakening silent biosynthetic gene clusters and linking orphan clusters to natural products in microorganisms. *Current Opinion in Chemical Biology*, *15*(1), 137–143.

https://doi.org/10.1016/j.cbpa.2010.10.011

Corbeski, I., Guo, X., Eckhardt, B. V., Fasci, D., Wiegant, W. W., Graewert, M. A., Vreeken, K., Wienk, H., Svergun, D. I., Heck, A. J. R., Van Attikum, H., Boelens, R., Sixma, T. K., Mattiroli, F., & Van Ingen, H. (2022). Chaperoning of the histone octamer by the acidic domain of DNA repair factor APLF. *Science Advances*, *8*(30). https://doi.org/10.1126/sciadv.abo0517

Cowan, M. M. (1999). Plant products as antimicrobial agents. *Clinical Microbiology Reviews*, *12*(4), 564–582. https://doi.org/10.1128/cmr.12.4.564

D'Costa, V. M., King, C., Kalan, L., Morar, M., Sung, W. W. L., Schwarz, C., Froese, D. G., Zazula, G. D., Calmels, F., Debruyne, R., Golding, G. B., Poinar, H. N., & Wright, G. D. (2011). Antibiotic resistance is ancient. *Nature*, *477*(7365), 457–461. https://doi.org/10.1038/nature10388

DDC. (2015). District Development Plan, Ilam. Government of Nepal, Ministry of Federal Affairs and Local Development, District Development Committee Office, Ilam, Nepal.

De Los Ángeles Quinteros, M., Martínez, I. M. A., Dalmasso, P. R., & Páez, P. L. (2016). Silver Nanoparticles: Biosynthesis Using an ATCC Reference Strain ofPseudomonas aeruginosaand Activity as Broad Spectrum Clinical Antibacterial Agents. *International Journal of Biomaterials*, *2016*, 1–7. https://doi.org/10.1155/2016/5971047

Dembicka, K. M., Powell, J., O'Connell, N. H., Hennessy, N., Brennan, G. I., & Dunne, C. P. (2021). Prevalence of linezolid-resistant organisms among patients admitted to a tertiary hospital for critical care or dialysis. *Irish Journal of Medical Science (1971 -)*, *191*(4), 1745–1750. https://doi.org/10.1007/s11845-021-02773-2

Dortet, L., Glaser, P., Kassis-Chikhani, N., Girlich, D., Ichaı, P., Boudon, M., Samuel, D., Creton, E., Imanci, D., Bonnin, R. A., Fortineau, N., & Naas, T. (2017). Long-lasting successful dissemination of resistance to oxazolidinones in MDR Staphylococcus epidermidis clinical isolates in a tertiary care hospital in France. *Journal of Antimicrobial Chemotherapy*, *73*(1), 41–51. https://doi.org/10.1093/jac/dkx370

Durán, N., Nakazato, G., & Seabra, A. B. (2016). Antimicrobial activity of biogenic silver nanoparticles, and silver chloride nanoparticles: an overview and comments. *Applied microbiology and biotechnology*, *100*, 6555-6570.

Durand, G., Raoult, D., & Dubourg, G. (2019). Antibiotic discovery: history, methods and perspectives. *International Journal of Antimicrobial Agents*, *53*(4), 371–382. https://doi.org/10.1016/j.ijantimicag.2018.11.010

Ekici, Ö. D., Paetzel, M., & Dalbey, R. E. (2008). Unconventional serine proteases: Variations on the catalytic Ser/His/Asp triad configuration. *Protein Science*, *17*(12), 2023–2037. https://doi.org/10.1110/ps.035436.108

Elshikh, M. S., Ahmed, S. M., Funston, S. J., Dunlop, P., McGaw, M., Marchant, R., & Banat, I. M. (2016). Resazurin-based 96-well plate microdilution method for the determination of minimum inhibitory concentration of biosurfactants. *Biotechnology Letters*, *38*(6), 1015–1019. https://doi.org/10.1007/s10529-016-2079-2 (Elshikh et al., 2016)

Fan, J., Fu, A., & Zhang, L. (2019). Progress in molecular docking. *Quantitative Biology*, *7*(2), 83–

89. https://doi.org/10.1007/s40484-019-0172-y

Gimeno, A., Ojeda-Montes, M. J., Tomás-Hernández, S., Ceretó-Massagué, A., Beltrán-Debón, R., Mulero, M., Pujadas, G., & García-Vallvé, S. (2019). The light and dark sides of virtual screening: What is there to know? *International Journal of Molecular Sciences*, *20*(6), 1375. https://doi.org/10.3390/ijms20061375

Guengerich, F. P. (2022). Inhibition of Cytochrome P450 Enzymes by Drugs-Molecular Basis and Practical Applications. *Biomolecules & Therapeutics*, *30*(1), 1–18. https://doi.org/10.4062/biomolther.2021.102

Ilić, S., Konstantinović, S. S., Todorović, Z. B., Lazić, M. L., Veljković, V. B., Joković, N., & Radovanović, B. (2007). Characterization and antimicrobial activity of the bioactive metabolites in streptomycete isolates. *Microbiology*, *76*(4), 421–428. https://doi.org/10.1134/s0026261707040066 Ilić et al. (2007); Ilić et al. (2007)

Jacob, J. A., Mahal, H. S., Biswas, N., Mukherjee, T., & Kapoor, S. (2007). Role of phenol derivatives in the formation of silver nanoparticles. *Langmuir*, *24*(2), 528–533. https://doi.org/10.1021/la702073r

Jumper, J., Evans, R., Pritzel, A., Green, T., Figurnov, M., Ronneberger, O., Tunyasuvunakool, K., Bates, R., Žídek, A., Potapenko, A., Bridgland, A., Meyer, C., Kohl, S. a. A., Ballard, A. J., Cowie, A., Romera-Paredes, B., Nikolov, S., Jain, R., Adler, J., . . . Hassabis, D. (2021). Highly accurate protein structure prediction with AlphaFold. *Nature*, *596*(7873), 583–589. https://doi.org/10.1038/s41586-021-03819-2

Kehrenberg, C., Aarestrup, F. M., & Schwarz, Š. (2007). IS 21-558 Insertion Sequences Are Involved in the Mobility of the Multiresistance Gene cfr. *Antimicrobial Agents and Chemotherapy*, *51*(2), 483–487. https://doi.org/10.1128/aac.01340-06

Kesharwani, P., Gorain, B., Low, S. Y., Tan, S., Ling, E. C. S., Lim, Y. K., Chin, C. M., Lee, P. Y., Lee, C. M., Ooi, C. H., Choudhury, H., & Pandey, M. (2018). Nanotechnology based approaches for anti-diabetic drugs delivery. *Diabetes Research and Clinical Practice*, *136*, 52–77. https://doi.org/10.1016/j.diabres.2017.11.018

Khorrami, S., Zarrabi, A., Khaleghi, M., Danaei, M., & Mozafari, M. R. (2018). Selective cytotoxicity of green synthesized silver nanoparticles against the MCF-7 tumor cell line and their enhanced antioxidant and antimicrobial properties. *International Journal of Nanomedicine*, *Volume 13*, 8013–8024. https://doi.org/10.2147/ijn.s189295

Kieser, T., Bibb, M. J., Buttner, M. J., Chater, K. F., & Hopwood, D. A. (2000). *Practical streptomyces genetics* (Vol. 291, p. 397). Norwich: John Innes Foundation.

Kotha, S. R., & Staller, M. V. (2023). Clusters of acidic and hydrophobic residues can predict acidic transcriptional activation domains from protein sequence. *Genetics*, *225*(2). https://doi.org/10.1093/genetics/iyad131

Kourkouta, L., Koukourikos, K., Iliadis, C., Plati, P., & Dimitriadou, A. (2018). History of antibiotics. *Sumerian J Med Healthcare*, *1*, 51-5.

Kumar, A., & Jha, A. (2017). Drug development Strategies. In *Elsevier eBooks* (pp. 63–71).

https://doi.org/10.1016/b978-0-12-811311-0.00007-7

Kumar, S., Saikia, D., & Kumar, H. (2023). Impact of COVID-19 on drug discovery and Development: A pharmacologist's perspective. *Advanced Biomedical Research*, *12*(1), 212. https://doi.org/10.4103/abr.abr_174_23

Lawson, B. R., Eleftheriadis, T., Tardif, V., González-Quintial, R., Baccalà, R., Kono, D. H., & Theofilopoulos, A. N. (2012). Transmethylation in immunity and autoimmunity. *Clinical Immunology*, *143*(1), 8–21. https://doi.org/10.1016/j.clim.2011.10.007

Lee, L., Goh, B. H., & Chan, K. (2020). Editorial: Actinobacteria: Prolific Producers of Bioactive Metabolites. *Frontiers in Microbiology*, *11*. https://doi.org/10.3389/fmicb.2020.01612

Lee, S. M., Song, K. C., & Lee, B. S. (2010). Antibacterial activity of silver nanoparticles prepared by a chemical reduction method. *Korean Journal of Chemical Engineering*, *27*(2), 688–692. https://doi.org/10.1007/s11814-010-0067-0

Lewis, K. (2020). The Science of antibiotic Discovery. *Cell*, *181*(1), 29–45. https://doi.org/10.1016/j.cell.2020.02.056 (Lewis, 2020)

Liang, Z., & Li, Q. X. (2018). Π–Cation interactions in Molecular Recognition: Perspectives on Pharmaceuticals and pesticides. *Journal of Agricultural and Food Chemistry*, *66*(13), 3315–3323. https://doi.org/10.1021/acs.jafc.8b00758

Liato, V., & Aïder, M. (2017). Geosmin as a source of the earthy-musty smell in fruits, vegetables and water: Origins, impact on foods and water, and review of the removing techniques. *Chemosphere*, *181*, 9–18. https://doi.org/10.1016/j.chemosphere.2017.04.039

Libretexts. (2020, November 3). *Infrared Spectroscopy Absorption Table*. Chemistry LibreTexts. https://chem.libretexts.org/@go/page/22645?pdf

Lipinski, C. A., Lombardo, F., Dominy, B. W., & Feeney, P. J. (1997a). Experimental and computational approaches to estimate solubility and permeability in drug discovery and development settings. *Advanced Drug Delivery Reviews*, *23*(1–3), 3–25. https://doi.org/10.1016/s0169-409x(96)00423-1

Li, W., Yang, Z., Hu, J., Wang, B., Rong, H., Li, Z., Sun, Y., Wang, Y., Zhang, X., Wang, M., & Xu, H. (2022). Evaluation of culturable 'last-resort' antibiotic resistant pathogens in hospital wastewater and implications on the risks of nosocomial antimicrobial resistance prevalence. *Journal of Hazardous Materials*, *438*, 129477. https://doi.org/10.1016/j.jhazmat.2022.129477

Long, K. S., Poehlsgaard, J., Kehrenberg, C., Schwarz, Š., & Vester, B. (2006). The CFR RRNA methyltransferase confers resistance to phenicols, lincosamides, oxazolidinones, pleuromutilins, and streptogramin A antibiotics. *Antimicrobial Agents and Chemotherapy*, *50*(7), 2500–2505. https://doi.org/10.1128/aac.00131-06

Mahesh, S., Tang, K., & Raj, M. (2018). Amide bond activation of biological molecules. *Molecules (Basel. Online)*, *23*(10), 2615. https://doi.org/10.3390/molecules23102615

Mato, J. M., Álvarez, L., Ortiz, P., & Pajares, M. A. (1997). S-adenosylmethionine synthesis:

Molecular mechanisms and clinical implications. *Pharmacology & Therapeutics*, *73*(3), 265–280. https://doi.org/10.1016/s0163-7258(96)00197-0

Mendes, R. E., Deshpande, L. M., & Jones, R. N. (2014). Linezolid update: Stable in vitro activity following more than a decade of clinical use and summary of associated resistance mechanisms. *Drug Resistance Updates*, *17*(1–2), 1–12. https://doi.org/10.1016/j.drup.2014.04.002

Moo, C., Yang, S., Yusoff, K., Ajat, M., Thomas, W., Abushelaibi, A., Lim, S. H. E., & Lai, K. (2020). Mechanisms of antimicrobial resistance (AMR) and alternative approaches to overcome AMR. *Current Drug Discovery Technologies*, *17*(4), 430–447. https://doi.org/10.2174/1570163816666190304122219

Morgan, S., Grootendorst, P., Lexchin, J., Cunningham, C., & Greyson, D. (2011). The cost of drug development: A systematic review. *Health Policy*, *100*(1), 4–17. https://doi.org/10.1016/j.healthpol.2010.12.002

Morris, G. M., & Lim-Wilby, M. S. (2008). Molecular docking. In *Methods in molecular biology* (pp. 365–382). https://doi.org/10.1007/978-1-59745-177-2_19

Mulvaney, P. (1996). Surface plasmon spectroscopy of nanosized metal particles. *Langmuir*, *12*(3), 788–800. https://doi.org/10.1021/la9502711

O'Boyle, N. M., Banck, M., James, C. A., Morley, C., Vandermeersch, T., & Hutchison, G. (2011). Open Babel: An open chemical toolbox. *Journal of Cheminformatics*, *3*(1). https://doi.org/10.1186/1758-2946-3-33

Oli, A. K., Shivshetty, N., Kelmani, C. R., & Biradar, P. A. (2021). Actinomycetes in medical and pharmaceutical industries. In *Rhizosphere biology* (pp. 291–320). https://doi.org/10.1007/978-981-16-3353-9_16

Oves, M., Aslam, M., Rauf, M. A., Qayyum, S., Qari, H. A., Khan, M. S., Alam, M. Z., Tabrez, S., Pugazhendhi, A., & Ismail, I. M. (2018). Antimicrobial and anticancer activities of silver nanoparticles synthesized from the root hair extract of Phoenix dactylifera. *Materials Science and Engineering: C*, *89*, 429–443. https://doi.org/10.1016/j.msec.2018.03.035

Pagadala, N. S., Syed, K., & Tuszyński, J. A. (2017). Software for molecular docking: a review. *Biophysical Reviews*, *9*(2), 91–102. https://doi.org/10.1007/s12551-016-0247-1

Papp-Wallace, K. M., Endimiani, A., Taracila, M. A., & Bonomo, R. A. (2011). Carbapenems: past, present, and future. *Antimicrobial Agents and Chemotherapy*, *55*(11), 4943–4960. https://doi.org/10.1128/aac.00296-11

Park, M. H., & Igarashi, K. (2013). Polyamines and their metabolites as diagnostic markers of human diseases. *Biomolecules & Therapeutics*, *21*(1), 1–9. https://doi.org/10.4062/biomolther.2012.097

Parveen, K., Banse, V., & Ledwani, L. (2016, April). Green synthesis of nanoparticles: Their advantages and disadvantages. In *AIP conference proceedings* (Vol. 1724, No. 1). AIP Publishing.

Patil, R. R., Das, S., Stanley, A., Yadav, L., Sudhakar, A., & Varma, A. K. (2010). Optimized hydrophobic interactions and hydrogen bonding at the Target-Ligand interface leads the pathways of Drug-Designing. *PLOS ONE*, *5*(8), e12029. https://doi.org/10.1371/journal.pone.0012029

Pérez-Sala, D., Martínez-Costa, Ó. H., Aragón, J. L., & Pajares, M. A. (2018). Alterations in nucleocytoplasmic localization of the methionine cycle induced by oxidative stress during liver disease. In *Elsevier eBooks* (pp. 21–41). https://doi.org/10.1016/b978-0-12-803951-9.00003-3

Polgár, L. (2005). The catalytic triad of serine peptidases. *Cellular and Molecular Life Sciences*, *62*(19–20), 2161–2172. https://doi.org/10.1007/s00018-005-5160-x

Polikanov, Y. S., Starosta, A. L., Juette, M. F., Altman, R. B., Terry, D. S., Lu, W., Burnett, B., Dinos, G. P., Reynolds, K. A., Blanchard, S. C., Steitz, T. A., & Wilson, D. N. (2015). Distinct tRNA Accommodation Intermediates Observed on the Ribosome with the Antibiotics Hygromycin A and A201A. *Molecular Cell*, *58*(5), 832–844. https://doi.org/10.1016/j.molcel.2015.04.014

Präbst, K., Engelhardt, H., Ringgeler, S., & Hübner, H. (2017). Basic colorimetric proliferation assays: MTT, WST, and Resazurin. In *Methods in molecular biology* (pp. 1–17). https://doi.org/10.1007/978-1-4939-6960-9_1

Price, M. N., Dehal, P., & Arkin, A. P. (2010). FastTree 2 – approximately Maximum-Likelihood trees for large alignments. *PLOS ONE*, *5*(3), e9490. https://doi.org/10.1371/journal.pone.0009490

Qian, S. B., Waldron, L., Choudhary, N., Klevit, R. E., Chazin, W. J., & Patterson, C. (2009). Engineering a ubiquitin ligase reveals conformational flexibility required for ubiquitin transfer. *Journal of Biological Chemistry*, *284*(39), 26797–26802. https://doi.org/10.1074/jbc.m109.032334

Quinn, G. A., Banat, A. M., Abdelhameed, A., & Banat, İ. M. (2020). Streptomyces from traditional medicine: sources of new innovations in antibiotic discovery. *Journal of Medical Microbiology*, *69*(8), 1040–1048. https://doi.org/10.1099/jmm.0.001232

Ranaghan, K. E., Hung, J. E., Bartlett, G. J., Mooibroek, T. J., Harvey, J. N., Woolfson, D. N., Van Der Donk, W. A., & Mulholland, A. J. (2014). A catalytic role for methionine revealed by a combination of computation and experiments on phosphite dehydrogenase. *Chemical Science*, *5*(6), 2191–2199. https://doi.org/10.1039/c3sc53009d

Rijal, K. R., Banjara, M. R., Dhungel, B., Kafle, S., Gautam, K. R., Ghimire, B., Ghimire, P., Dhungel, S., Adhikari, N., Shrestha, U. T., Sunuwar, D. R., Adhikari, B., & Ghimire, P. (2021). Use of antimicrobials and antimicrobial resistance in Nepal: a nationwide survey. *Scientific Reports*, *11*(1). https://doi.org/10.1038/s41598-021-90812-4

Riss, T. L., Moravec, R. A., Niles, A. L., Duellman, S., Benink, H. A., Worzella, T. J., & Minor, L. (2016). Cell viability assays. *Assay Guidance Manual [Internet]*.

Roopashree, K. M., & Naik, D. (2019). Advanced method of secondary metabolite extraction and quality analysis. *Journal of Pharmacognosy and Phytochemistry*, *8*(3), 1829-1842.

Sah, S. N., Majhi, R., Regmi, S., Ghimire, A., Biswas, B., Yadav, L. P., Sah, R., & Shah, P. K. (2021).

Fermentation and Extraction of Antibacterial Metabolite Using Streptomyces spp. Isolated from Taplejung, Nepal. *Journal of Institute of Science and Technology*, *26*(1), 8–15. https://doi.org/10.3126/jist.v26i1.37808 (Sah et al., 2021)

Sander, T., Freyss, J., Von Korff, M., & Rufener, C. (2015). DataWarrior: an Open-Source program for chemistry aware data visualization and analysis. *Journal of Chemical Information and Modeling*, *55*(2), 460–473. https://doi.org/10.1021/ci500588j

Schaenzer, A. J., Hernández, Á. R., Tsai, K., Hobson, C., Fujimori, D. G., & Wright, G. D. (2023). Angucyclinones rescue PhLOPS A antibiotic activity by inhibiting Cfr-dependent antibiotic resistance. *MBio*, *14*(6). https://doi.org/10.1128/mbio.01791-23

Schinkel, C. C. F., Kirchheimer, B., Dellinger, A. S., Klatt, S., Winkler, M., Dullinger, S., & Hörandl, E. (2015). Correlations of polyploidy and apomixis with elevation and associated environmental gradients in an alpine plant. *Aob Plants*, *8*. https://doi.org/10.1093/aobpla/plw064

Smith, L. K., & Mankin, A. S. (2008). Transcriptional and Translational Control of the mlr Operon, Which Confers Resistance to Seven Classes of Protein Synthesis Inhibitors. *Antimicrobial Agents and Chemotherapy*, *52*(5), 1703–1712. https://doi.org/10.1128/aac.01583-07

Souri, N., Abbaszadeh, M., & Ghorbanzadeh, S. (2023). Colorimetric detector for hydrogen sulfide detection in industrial environments based on silver nanoparticles synthesized in streptomyces bacteria. *bioRxiv (Cold Spring Harbor Laboratory)*. https://doi.org/10.1101/2023.01.25.525489

Sumitha, A., Devi, P. B., Hari, S., & Dhanasekaran, R. (2020). Covid-19 - In Silico Structure Prediction and Molecular Docking Studies with Doxycycline and Quinine. *Biomedical and Pharmacology Journal*, *13*(03), 1185–1193. https://doi.org/10.13005/bpj/1986

Takahashi, Y., & Nakashima, T. (2018). Actinomycetes, an inexhaustible source of naturally occurring antibiotics. *Antibiotics*, *7*(2), 45. https://doi.org/10.3390/antibiotics7020045

Tiwari, K., & Gupta, R. K. (2011). Rare actinomycetes: a potential storehouse for novel antibiotics. *Critical Reviews in Biotechnology*, *32*(2), 108–132. https://doi.org/10.3109/07388551.2011.562482

Tiwari, A., & Singh, S. (2022). Computational approaches in drug designing. In *Elsevier eBooks* (pp. 207–217). https://doi.org/10.1016/b978-0-323-89775-4.00010-9

Tooke, C., Hinchliffe, P., Bragginton, E. C., Colenso, C. K., Hirvonen, V. H. A., Takebayashi, Y., & Spencer, J. (2019). B-Lactamases and B-Lactamase inhibitors in the 21st century. *Journal of Molecular Biology*, *431*(18), 3472–3500. https://doi.org/10.1016/j.jmb.2019.04.002

Tôrres, P., Sodero, A. C. R., Jofily, P., & Silva, F. P. (2019). Key topics in Molecular Docking for Drug Design. *International Journal of Molecular Sciences*, *20*(18), 4574. https://doi.org/10.3390/ijms20184574

Tsai, K., Stojković, V., Noda-Garcia, L., Young, I., Myasnikov, A. G., Kleinman, J., Palla, A., Floor, S. N., Frost, A., Fraser, J. S., Tawfik, D. S., & Fujimori, D. G. (2022). Directed evolution of the rRNA methylating enzyme Cfr reveals molecular basis of antibiotic resistance. *eLife (Cambridge)*, *11*. https://doi.org/10.7554/elife.70017

Tsiodras, S., Gold, H. S., Sakoulas, G., Eliopoulos, G. M., Wennersten, C., Venkataraman, L., Moellering, R. C., & Ferraro, M. J. (2001). Linezolid resistance in a clinical isolate of Staphylococcus aureus. *The Lancet*, *358*(9277), 207–208. https://doi.org/10.1016/s0140-6736(01)05410-1

Van Norman, G. A. (2016). Drugs, Devices, and the FDA: Part 1. *JACC: Basic to Translational Science*, *1*(3), 170–179. https://doi.org/10.1016/j.jacbts.2016.03.002 (Van Norman, 2016)

Veber, D. F., Johnson, S. R., Cheng, H., Smith, B. R., Ward, K. W., & Kopple, K. D. (2002). Molecular properties that influence the oral bioavailability of drug candidates. *Journal of Medicinal Chemistry*, *45*(12), 2615–2623. https://doi.org/10.1021/jm020017n

Williams, S. T., & Vickers, J. C. (1988). Detection of actinomycetes in the natural environment: problems and perspectives. *Biology of actinomycetes*, *88*, 265-270.

World Health Organization. (2019). Critically important antimicrobials for human medicine. Pg (24)

World Health Organization: WHO. (2017, February 27). WHO publishes list of bacteria for which new antibiotics are urgently needed. *www.who.int*. Retrieved January 2, 2023, from https://www.who.int/news/item/27-02-2017-who-publishes-list-of-bacteria-for-which-new-antibiotics-are-urgently-needed

Wypij, M., Czarnecka, J., Świecimska, M., Dahm, H., Rai, M., & Golińska, P. (2018). Synthesis, characterization and evaluation of antimicrobial and cytotoxic activities of biogenic silver nanoparticles synthesized from Streptomyces xinghaiensis OF1 strain. *World Journal of Microbiology & Biotechnology*, *34*(2). https://doi.org/10.1007/s11274-017-2406-3 (Wypij et al., 2018), Wypij et al. (2018)

Yang, L. (2003). Different alterations of cytochrome P450 3A4 isoform and its gene expression in livers of patients with chronic liver diseases. *World Journal of Gastroenterology*, *9*(2), 359. https://doi.org/10.3748/wjg.v9.i2.359

Yin, I. X., Zhang, J., Zhao, I. S., Mei, M. L., Li, Q., & Chu, C. H. (2020). The Antibacterial Mechanism of Silver Nanoparticles and Its Application in Dentistry. *International Journal of Nanomedicine*, *Volume 15*, 2555–2562. https://doi.org/10.2147/ijn.s246764

Zargoosh, Z., Ghavam, M., Bacchetta, G., & Tavili, A. (2019). Effects of ecological factors on the antioxidant potential and total phenol content of Scrophularia striata Boiss. *Scientific Reports*, *9*(1). https://doi.org/10.1038/s41598-019-52605-8

Zheng, J., Chen, S., Song, M., Liu, B. L., Ma, S., Wang, S., Wang, Q., Ding, Q., Xia, Q., Zhu, K., & Wang, H. (2024). Discovery of adjuvants with antibacterial potentiation activity against carbapenemase-producing Enterobacterales based on in silico virtual screening. *International Journal of Antimicrobial Agents*, *63*(2), 107076. https://doi.org/10.1016/j.ijantimicag.2023.107076

Zheng, S., Lei, Z., Ai, H., Chen, H., Deng, D., & Yang, Y. (2021). Deep scaffold hopping with multimodal transformer neural networks. *Journal of Cheminformatics*, *13*(1). https://doi.org/10.1186/s13321-021-00565-5

APPENDICES

Web site visited

Rcsb	https://www.rcsb.org/
AlphaFold	https://alphafold.ebi.ac.uk/
ProSA-web	https://prosa.services.came.sbg.ac.at/prosa.php
Uniprot	https://www.uniprot.org/
NCBI	https://www.ncbi.nlm.nih.gov/

Compositions

Acidic $HgCl_2$ solution
15g $HgCl_2$ in 20ml HCl
final volume maintained by 100ml distil water

Carbohydrate broth (peptone- 1%, Sodium chloride- 0.5%, phenol red 0.005%, distilled water-

100ml, pH-7.8, carbohydrate- 0.5%

Phenol red- red at 8.5, yellow at pH 6.9

Nitrate test

Reagent A: 0.5g alpha-naphthylamine (a carcinogen) in 100ml 5N acetic acid.

5N acetic acid = 28.7ml GAA (17.4N) final vol. of 100ml.

Reagent B: 0.8g sulfanilic acid in 100ml 5N acetic acid by gently heating.

Reagent C: 1g alpha-naphthol in 200ml acetic acid.

American Type Culture Collection (ATCC) bacteria
Staph 29213/ 43300
E. coli. 25922
K. Pneumoniae 700603

Resazurin
1% resazurin stock (0.01gm in 1ml = 10mg/ml)
15µl (resazurin stock solution) + 985µl (H_2O) = 0.15mg/ml resazurin (0.015%)
20µl (0.15mg/ml) resazurin
2.5 to 3.5 hr incubation at 37^0C.

$AgNO_3$
1mM/L = 0.001 M/L
Stock AgNO3 = 10mM; Final= 1mM

TAE (50X)
242 gm t5ris-base on dd H_2O
57.1 ml Glacial acetic acid
100ml 0.5M EDTA (pH=8) solution
Adjust volume. to 1L.

Stach Casein Broth (SCB)
Soluble starch- 10g, casein (vit. free)- 0.3g, KNO_3- 2g, $MgSO_4.7H_2O$ – 0.05g, K_2HPO_4- 2g, NaCl- 2g, $CaCO_3$- 0.02g, $FeSO_4.7H_2O$- 0.01g, dd H_2O- 1000ml.; pH (at 25^0C) = 7.0 +- 0.1

ISP4 media
Soluble starch- 10g, $MgSO_4.7H_2O$ – 1g, NaCl- 1g, $(NH_4)_2SO_4$- 2g, $CaCO_3$- 2g,
1ml trace salts solution

- $FeSO_4.7H_2O$- 0.1g,
- $MnCl_2.4H_2O$- 0.1g,
- $ZnSO_4.7H_2O$- 0.1g in 100ml

Final volume adjusted by dd H_2O- 1000ml.;
pH (at 25^0C) = 7.0 to 7.4

Sequence Data